PERFORMANCE ANALYSIS OF COOPERATIVE COMMUNICATION SYSTEMS WITH IMPERFECT CHANNEL STATE INFORMATION

by

Mohammad Jafar Taghiyar Renani

B.Sc, Isfahan University of Technology, Isfahan, Iran, 2008

A Thesis submitted in partial fulfillment
of the requirements for the degree of
Master of Applied Science
in the School
of
Engineering Science

SIMON FRASER UNIVERSITY
Spring 2011

APPROVAL

Name: Mohammad Jafar Taghiyar Renani

Degree: Master of Applied Science

Title of Thesis: Performance Analysis of Cooperative Communication Systems with Imperfect Channel State Information

Examining Committee:

Dr. Paul Ho, P. Eng
Professor, School of Engineering Science
Chair

Dr. Sami Muhaidat
Co-Senior Supervisor
Assistant Professor, School of Engineering Science

Dr. Jie Liang, P. Eng
Co-Senior Supervisor
Assistant Professor, School of Engineering Science

Dr. Atousa HajShirMohammadi, P. Eng
Internal Examiner
Senior Lecturer, School of Engineering Science

Date Approved: January 24, 2011

Declaration of
Partial Copyright Licence

Abstract

Space-time coding has demonstrated that the deployment of multiple antennas at the transmitter allows for simultaneous increase in throughput and reliability. However, the use of antenna arrays is impractical for deployment in some practical scenarios. Therefore, cooperative diversity has been recently introduced for realizing transmit diversity.

Most of the literature in cooperative diversity assume perfect channel state information (CSI). However, in practice, imperfect CSI should be considered. In this thesis, we first investigate the performance of cooperative communications with imperfect CSI, where the channel estimates are obtained by pilot symbols. We present an exact bit error probability expression in the presence of channel estimation errors.

We also study the effect of imperfect CSI in two-way multi-relay cooperative networks when the max-min relay selection is used. We derive an exact expression for the outage probability based on which a novel optimum power allocation scheme is proposed.

Keywords: Cooperative communications, Diversity, Imperfect channel state information, Outage probability, Relay selection, Two-way relaying networks.

Dedication

To my dearest parents.

Acknowledgments

I am indebted to many for helping me during my graduate study and development of this thesis.

Greatest gratitude goes to my advisors, Dr. Sami Muhaidat and Dr. Jie Liang who have been a tremendous source of inspiration, guidance, and encouragement. I have extremely benefited from the invaluable freedom they have provided, the thoughtful advices they have given, and the fruitful interactions they have offered.

The friendly and energetic environment of the Simon Fraser university and in particular, the MCL group, has provided me with a wonderful opportunity to build my graduate life. Special thanks go to Mehdi Seyfi, Homa Eghbali, Jing Wang, and Xiaoyu Xiu for their help and lively discussions on research.

I am also greatly thankful to Sara Sadeghi for her all invaluable supports.

I would also like to thank Dr. Atousa HajShirMohammadi for her precise review and meticulous comments and Prof. Paul Ho for spending his valuable time to chair my defense.

And finally, my whole student career has been impossible without the support and encouragement of my family. My warmest feelings and deepest thanks are for my Dad, Mom, Sisters and Brother.

Contents

List of Tables

List of Figures

Notations

$f_X(x)$	Probability density function
$F_X(x)$	Cumulative distribution function
$\mathcal{E}[.]$	Mathematical expectation operator
$\mathcal{CN} \sim (\mu, \sigma^2)$	Complex Gaussian distribution with mean μ and variance σ^2
$Q(x)$	Standard cumulative distribution function
ρ	Correlation coefficient
η	Amplifying coefficient at relay terminals in AaF relaying mode
$h_{i,j}$	Channel gains
$\hat{h}_{i,j}$	Estimated channel gains
d	An auxiliary zero-mean complex Gaussian random variable
n	AWGN channel noise
$(.)^*$	Conjugate operator
$(.)^H$	Hermitian transpose operator
E	Transmitted power
r	Received signal
R	Relay terminal
S	Source terminal
D	Destination terminal
$A \rightarrow B$	A to B link

Chapter 1

Introduction

1.1 Thesis motivation

The demand for higher transmission rates and better quality of service in wireless communications systems continues to escalate. The emerging fourth-generation (4G) technologies such as WiMAX and long-term evolution (LTE) Advanced are promised to significantly improve the performance of wireless systems. The 4th generation systems are envisioned to accommodate and integrate all existing and future technologies in a single standard. One of the key features of the 4G systems would be *high usability* [1], i.e., the user would be able to use the system at anytime, anywhere, and with any technology. Users carrying an integrated wireless terminal would have access to a variety of multimedia applications in a reliable environment at lower cost. To meet these demands, next generation wireless communication systems must support high capacity with high bandwidth efficiency to conserve limited spectrum resources. Utilizing multiple antennas is another key feature to these technologies which can help increase the system capacity and reliability.

Cooperative wireless communications exploits the virtual antenna array formed with multiple relays, instead of actually deploying multiple antennas, to generate spatial diversity. Cooperative spatial diversity is a promising technique that can be applied to extend the coverage or increase the system capacity. The pioneering works in this area address mainly information theoretic aspects, deriving fundamental performance bounds. However, practical implementation of cooperative diversity requires an in-depth investigation of several physical layer issues such as channel estimation, equalization, and synchronization integrating the underlying cooperation protocols and relaying modes. Moreover, most of the current

literature in this area assume an idealized transmission environment with an underlying flat frequency fading channel model and perfect channel state information (CSI) which can be far away from being realistic for different wireless applications.

Motivated by the aforementioned practical impairments, the main purpose of this thesis is to investigate the impact of imperfect channel state information for different channel models and developing an insight to the performance of cooperative diversity networks.

1.2 Outline and Main Contributions

In Chapter 2, we provide a brief review of important background materials related to the thesis. We first review different diversity techniques for fading channels including time diversity, frequency diversity, and space diversity, followed by an introduction to different diversity combining techniques. We then introduce some important concepts that will be used extensively throughout the thesis, including transmit diversity, space-time coding, cooperative diversity, and channel models with imperfect CSI.

In Chapter 3, we analyze the performance of pilot symbol assisted modulation (PSAM) scheme used in a relay-assisted space-time block coded (STBC) network that operates in amplify-and-forward (AaF) mode. We derive the correlation coefficients of the fading channel gains and their estimates for both fading and non-fading $R \rightarrow D$ link. It is shown that the presence of fading in the $R \rightarrow D$ link manifests itself with the introduction of additional Doppler frequency terms. We further express the bit error probability (BEP) in terms of Doppler frequency, number of pilot symbols and signal-to-noise ratio (SNR) when the estimation via PSAM scheme is not perfect.

Analog network coding (ANC) and physical layer network coding (PLNC) [2, 3] are efficient ways to improve the bandwidth efficiency of the two-way relay networks, where two terminals want to send information to each other via the help of some relay terminals located between them by exploiting cooperative communications technique. They can shorten one round information exchange into two time-slots by allowing signal collision at the relay terminals. In ANC scheme, relay terminals carry on some linear operations to the received mixed analog signals from both terminals and then broadcast them back to the destination terminals. Each terminal can subtract the backward self-interference signal from itself and obtain the signal from the other one.

Obviously, the best performance is achieved when the channel state information (CSI)

is perfect, but this is unrealistic in practical scenarios. The channel coefficients must be estimated and then used in the detection process [4]. Therefore, it is of importance to investigate the effect of estimation errors on the performance of two-way cooperative systems. Chapter 4 mainly explores the performance of max-min relay selection in two-way multi-relaying networks when no terminal in the system has the knowledge of perfect CSI.

Finally, we summarize the work in this thesis and present the concluding remarks and directions for future research in Chapter 5.

1.3 List of Publications

1. **M. J. Taghiyar**, S. Muhaidat, and J. Liang, "Relay selection in bidirectional cooperative networks with imperfect channel estimation," *Submitted to IEEE Trans. Wireless Commun.,* December 2010.

2. **M. J. Taghiyar**, S. Muhaidat, and J. Liang, "On Pilot-Symbol-Assisted Cooperative System with Cascaded Rayleigh and Rayleigh Fading Channels with Imperfect CSI," *J. Sel. Areas Telecommun. (JSAT),* November 2010.

3. **M. J. Taghiyar**, S. Muhaidat, and J. Liang, "On the Performance of Pilot Symbol Assisted Modulation for Cooperative Systems with Imperfect Channel Estimation," *in Proc. IEEE WCNC10,* Sydney, Australia, pp. 1-5, April 2010.

4. **M. J. Taghiyar**, M. seyfi, S. Muhaidat, and J. Liang, "Bidirectional Cooperative Systems with Outdated Channel State Information," *To be submitted.*

Chapter 2

Background

Wireless communications today covers a very wide array of applications and is one of the most active areas of technology. The characteristics of wireless channel impose fundamental limitations on the performance of wireless communication systems. The wireless channel characteristics can be investigated by dividing them into two parts, i.e., large-scale (long-term) impairments including path loss and shadowing, and small-scale (short-term) impairment which is commonly referred to as fading. The former component is used to predict the average signal power at the receiver side and the transmission coverage area. The latter is due to the multipath propagation which causes random fluctuations in the received signal level and affects the instantaneous SNR [5].

A common approach to mitigate the degrading effects of fading is the use of diversity techniques. Diversity improves transmission performance by making use of more than one independently faded version of the transmitted signal. If several replicas of the signals are transmitted over multiple channels that exhibit independent fading with comparable strengths, the probability that all the independently faded signal components experience deep fading simultaneously is significantly reduced.

This chapter reviews diversity techniques for fading channels as one of the essential tools to confront the effect of fading. It surveys different diversity combining techniques.

2.1 Diversity

To combat the detrimental effect of fading in wireless communications, independent copies of the transmitted signal are sent to the same destination over independent channels. Therefore, using an appropriate combining scheme at the receiver side enables the receiver to extract more information about the transmitted signal out of different versions of the received signals, even in the presence of destructive fading in the channel. There are various methods to exploit diversity from a wireless fading channel that are mainly classified as follow:

2.1.1 Time Diversity

In this form of diversity, the same signal is transmitted in different time slots separated by an interval longer than the coherence time of the channel, or by an interval reciprocal to the fading rate. Time diversity can usually be achieved via coding and interleaving. In other words, the transmitted signal is coded and then dispersed over time in different coherence periods. Interleaving of the resultant codewords is also required to ensure that the coded symbols are transmitted over independent fading gains [5]. In fast fading environments where the mobility is high, time diversity becomes very efficient. However, for slow fading channel e.g., low mobility environments and fixed-wireless applications, it offers little protection unless significant interleaving delays can be tolerated.

2.1.2 Frequency Diversity

In this form of diversity, the same signal is sent over different frequency carriers, whose separation must be larger than the coherence bandwidth of the channel to ensure independence among diversity channels. Since multiple frequencies are needed, this is generally not a bandwidth-efficient solution. This form of diversity is appropriate for indoor wireless communications, operating in frequency range 20-60 GHz where bandwidth is in abundance [6].

2.1.3 Space Diversity

Space diversity, also known as antenna diversity, is basically achieved by employing multiple antennas, thus producing independently faded versions of the transmitted signal at the

receiver [7]. To extract full diversity advantages, spacing between antenna elements should be wide enough with respect to the carrier wavelength. The required antenna separation depends on the local scattering environment as well as on the carrier frequency.

Since this form of diversity requires no extra bandwidth, and can be readily combined with other forms of diversity, in most scattering environments, spatial diversity is more practical and hence widely applied technique compared to the two previous forms of diversity.

Polarization diversity and *angle diversity* are also two forms of space diversity where in the former, horizontal and vertical polarization signals are transmitted via two different polarized antennas. The latter is usually applied for transmissions with carrier frequency larger than 10 GHz [6].

2.2 Diversity Combining Techniques

In the preceding section, differen diversity techniques were briefly introduced. A proper combination of various signal replicas provided at the receiver can greatly increase the instantaneous received signal-to-noise ratio (SNR), which in turn enhances the performance of the wireless communication system. The main types of combining techniques are *selection combining*, *switched combining*, *equal-gain combining* (EGC), and *maximal ratio combining* (MRC).

2.2.1 Selection Combining

Selection combining is one of the simplest combining methods where the signal with the largest instantaneous SNR is selected at every symbol interval. Since it requires only to measure the powers received form each path, it is relatively easy to implement. However, the information from the other branches is completely ignored which results in non-optimality of this technique.

2.2.2 Switch Combining

In switch combining, also known as scanning diversity, the receiver scans all the diversity branches and selects a particular branch with the SNR above a certain predetermined threshold. The signal is selected as the output until its SNR drops below the threshold. Once this happens, the receiver starts scanning again and switches to another branch. Compared

to selection combining, switch combining is inferior, since it does not continually select the best instantaneous SNR. Switch combining and selection combining do not require any knowledge of the channel state information. Therefore, they can be used in conjunction with coherent as well as non-coherent modulations.

2.2.3 Equal Gain Combining

Equal gain combining is a simple suboptimal linear combining method where the signal at the output of each branch is individually weighted by a coefficient equal to $e^{-j\phi_i}$ where ϕ_i is the phase of each received signal, and then added together to get the output signal. The amplitude of all received signals is set to unity, resulting in a loss of information in the amplitude. This technique outperforms the other previous two techniques.

2.2.4 Maximal Ratio Combining

Maximal ratio combining is also a linear combining method. In this technique, the signals at the output of diversity branches are again combined linearly and the coefficients of the linear combination are selected to maximize the SNR regarding both the phase and the amplitude.

This technique makes use of the both fading amplitude and phase information of all various received signals and thus outperforms all the aforementioned combining techniques. However, the implementation complexity of the EGC is significantly less than MRC. Furthermore, since this scheme requires the knowledge of channel fading amplitude and signal phase, it can only be used in conjunction with coherent detection.

2.3 Transmit Diversity

As mentioned in the preceding sections, using receive diversity brings about diversity gain which is used to minimize the effect of fading. This technique has been successfully used in uplink transmission where the base station can be easily equipped with more than one antenna. However, in downlink transmission, due to the size, power, and cost limitations, it is impractical to deploy multiple antennas at the mobile terminals. Transmit diversity, i.e., use of multiple antennas at the transmitter, is thus proposed for the downlink transmission. Transmit diversity results in a simpler structure, lower power consumption and lower cost

at the receiver as well as a considerable increase in channel capacity.

There are two major classes of transmit diversity schemes, namely *open-loop* schemes and *closed-loop* scheme. In closed-loop schemes, a feedback link is used between transmitter and receiver. Closed-loop transmit diversity has more power efficiency compared to open-loop transmit diversity. However, it increases the overhead of transmission and therefore is not bandwidth-efficient. Moreover, in practice, vehicle movements or interferences cause a mismatch between the state of the channel perceived by the transmitter and that perceived by the receiver, making the feedback unreliable in some situations.

In open-loop transmit diversity schemes, no feedback is required. They use linear processing at the transmitter to spread the information across multiple antennas. At the receive side, information is recovered by either linear processing or maximum-likelihood decoding techniques. The first of such schemes was proposed by Wittneben [8] where the operating frequency-flat fading channel is converted intentionally into a frequency-selective channel to exploit artificial path diversity by means of a maximum-likelihood decoder. It was later shown in the literature that delay diversity schemes are optimal in providing diversity in the sense that the diversity advantage experienced by an optimal receiver is equal to the number of transmit antennas [8, 9, 10].

Space-time coding (STC) has also been introduced as a special class of transmit diversity. In the following, we first briefly review the concept of STC's. Then we discuss the simplest but one the most effective space-time block codes, the so-called Alamouti scheme.

2.3.1 Space-time coding

Coding for multiple antenna transmission is known as *space-time coding*. In this coding technique, the redundancy is inserted in both space and time domains. Due to joint design in two spaces, these codes can achieve transmit diversity as well as coding gain without sacrificing bandwidth [11].

Specifically, to describe the *space-time trellis coding* (STTC) technique, introduced by Tarokh *et al.* in [12], let $\mathbf{X}$ denotes the $W \times M$ codewords matrix where W is the codeword length and M is the total number of transmit antennas used to generate diversity. Each entry in $\mathbf{X}$ is the modulated symbol transmitted to the receiver. The received signal can be expressed as

$$\mathbf{R} = \mathbf{XH} + \mathbf{N}, \tag{2.1}$$

where $\mathbf{R}$ is the $W \times N$ received signal matrix, N is the number of antennas at the receiver. $\mathbf{H}$ is the channel matrix of size $M \times N$ and $\mathbf{N}$ is the AWGN noise matrix of size $W \times N$.

Now, defining $\mathbf{E} = (\mathbf{X} - \hat{\mathbf{X}})(\mathbf{X} - \hat{\mathbf{X}})^H$ as the codeword difference matrix where $\hat{\mathbf{X}}$ is the ML-detected codeword matrix at the receiver, the design criteria for space-time codes are stated as [12]:

Rank criterion The matrix $\mathbf{E}$, taken over all possible combinations of code matrices, should be full rank. This criterion ensures the maximum diversity gain that is equal to $\min\{W, M\}$.

Determinant criterion The determinant of matrix $\mathbf{E}$, taken over all possible combinations of code matrices, should be maximized which results in the maximum possible coding gain.

Based on these criteria the well-defined trellis codes were proposed in [12] where standard soft-decision decoding algorithms such as Viterbi decoder can readily be implemented at the receiver. However, the decoding complexity of STTC's increases exponentially with transmission rate when the number of transmit antennas is fixed. This motivates a search for a generalized Alamouti scheme that works for any number of transmit antenna while preserving the simplicity of decoding. Therefore, *space-time block code* (STBC) has been proposed by Tarokh, Jafarkhani and Calderbank in [13] as an attractive alternative to STTC based on the theory of orthogonal designs. These codes are defined by a mapping operation of a block of input symbols into the space and time domains, transmitting the resulting sequences from different antennas simultaneously. Since then, an intensive research on space-time cods has been done to further improve the data rate of STBC's among which we refer to [11, 14, 15] and references therein.

2.3.2 Alamouti Scheme

Prior to the proposal of Alamouti scheme, transmit diversity was studied extensively but no simple decoding scheme was proposed. In 1998, Tarokh *et.al.* proposed space-time trellis coding (STTC) in [12] to realize transmit diversity. In fact, space-time coding combines all the copies of the received signal in an optimal way to extract as much information from each of them as possible. However, the drawback of the decoding scheme of STC's is their exponentially increasing complexity as the transmission rate increases while the number of

transmit antennas is fixed. On the other hand, Alamouti proposed a remarkable though simple scheme for two transmit antennas based on block codes which is much less complex than STTC for two transmit antennas at the cost of a loss in performance compared to trellis codes [16]. The significance of Alamouti scheme is that it is the first demonstration of a method of encoding which enables full diversity with linear processing at the receiver. Furthermore, it is the first open-loop transmit diversity technique with this capability. This scheme also requires no bandwidth expansion, as redundancy is applied in space across multiple antennas, not in time or frequency. Subsequent generalizations of Alamouti scheme have led to a tremendous impact on the wireless communications industry and have been proposed in several third-generation standards.

Alamouti Two-Branch Transmit Diversity with One Receive Antenna

This scheme uses two transmit and one receive antennas. Assuming perfect channel state information at the receiver and that channel fading gains are constant during two symbol periods, the received signals are as follow

$$[r_1 \quad r_2] = [h_1 \quad h_2] \begin{pmatrix} x_1 & -x_2^* \\ x_2 & x_1^* \end{pmatrix} + [n_1 \quad n_2]. \tag{2.2}$$

In other words, at a given symbol interval, two data signals x_1 and x_2 are simultaneously transmitted from the first and the second transmit antennas, respectively. In the next symbol interval, $-x_2^*$ is transmitted from the first transmit antenna, and x_1^* is transmitted from the other transmit antenna. This technique, shown in Table 2.1, leads to encoding the data signals in spatial and temporal domain simultaneously *i.e.* space-time coding.

Table 2.1: The encoding and transmission sequence for Alamouti two-branch transmit diversity scheme

Time\Space	First transmit antenna	Second transmit antenna
First symbol interval	x_1	x_2
Second symbol interval	$-x_2^*$	x_1^*

Rewriting the received signals in terms of x_1 and x_2, we have

$$\begin{pmatrix} r_1 \\ r_2^* \end{pmatrix} = \underbrace{\begin{pmatrix} h_1 & h_2 \\ h_2^* & -h_1^* \end{pmatrix}}_{Y} \begin{pmatrix} x_1 \\ x_2 \end{pmatrix} + \begin{pmatrix} n_1 \\ n_2^* \end{pmatrix}. \tag{2.3}$$

One can easily verify that the columns of the channel gain matrix Y are orthogonal. So, the detection problem for x_1 and x_2 decomposes into two separate, orthogonal, scalar problems.

Using Alamouti combining scheme at the receiver terminal, the reconstructed data signals, $\hat{x}_1$ and $\hat{x}_2$, are given by [16]

$$\begin{pmatrix} \hat{x}_1 \\ \hat{x}_2 \end{pmatrix} = \begin{pmatrix} h_1^* & h_2 \\ h_2^* & -h_1 \end{pmatrix} \begin{pmatrix} r_1 \\ r_2^* \end{pmatrix}. \tag{2.4}$$

Substituting 2.3 into 2.4, thus gives the detected signals as

$$\hat{x}_1 = \left(|h_1|^2 + |h_2|^2\right) x_1 + h_1^* n_1 + h_2 n_2^*, \tag{2.5}$$

$$\hat{x}_2 = \left(|h_1|^2 + |h_2|^2\right) x_2 - h_1 n_2^* + h_2^* n_1. \tag{2.6}$$

The decision rule is based on ML detection where for each of the signals $\hat{x}_1$ and $\hat{x}_2$, it is expressed as follows for PSK signals [16]: for $j = 1, 2$, choose x_i iff

$$d^2(\hat{x}_j, x_i) \leq d^2(\hat{x}_j, x_k) \qquad \forall i \neq k. \tag{2.7}$$

The resulting combined signals in Alamouti combining scheme are equivalent to that obtained from two-branch MRC. The only difference is phase rotation on the noise components which does not degrade the effective SNR. Therefore, the obtained diversity order from Alamouti two-branch transmit diversity scheme with one receive antenna is equal to that of two-branch MRC.

Alamouti scheme can be generalized to two transmit and M receive antennas that results in a diversity order of $2M$. This may be applicable where multiple receive antennas at the remote units are feasible. The special case of two transmit and two receive antennas are discussed in the original paper [16]. The remarkable importance of Alamouti scheme with M receive antennas is that the combined signals from the two transmit antennas are the simple addition of the combined signals at each receive antenna. Therefore, to obtain the same diversity order as $2M$-branch MRC, one needs only to use the combiner of each receive antenna in the Alamouti scheme with two transmit and M receive antennas, and then simply add the combined signals from all the receive antennas.

2.4 Cooperative Communications

As mentioned in section 2.1, in order to mitigate the severity of fading phenomenon in wireless communications, diversity techniques are adopted. However, due to the size and/or power consumption of the mobile unit, it may not be possible to use multiple antennas to create space diversity. Cooperative communications, is a new approach to emulate spatial diversity by creating a virtual antenna array, whereby diversity gains are achieved via co-operation of other users as *relays*. Figure 2.1 shows a typical cooperative setting where two mobile terminals as source and destination communicate with each other. Each terminal is equipped with a single antenna and cannot individually generate diversity. However, some other mobile terminals can play the role of relays where they can forward some versions of *overheard information*, *i.e.* the information from the source terminal to the destination terminal as well as their own data. Since each path between every two terminals suffers a statistically independent fading, there will be different versions of data signal at the destination which consequently leads to diversity gain.

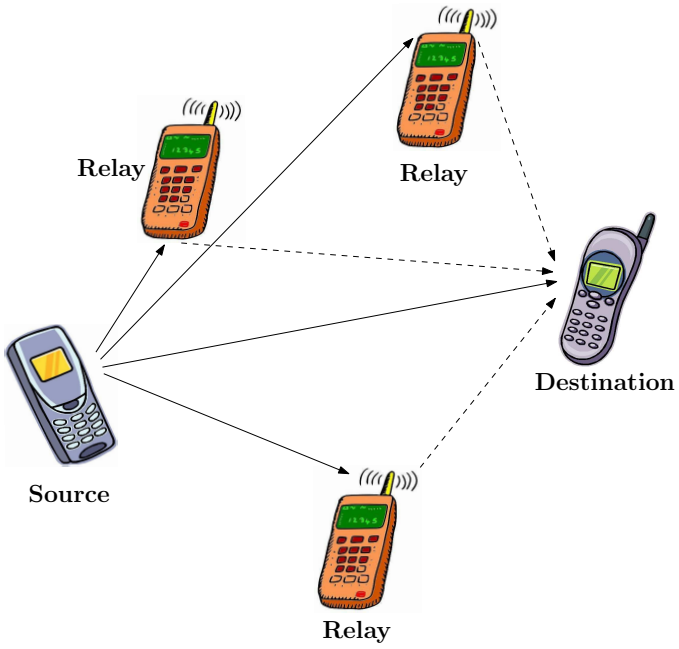

Figure 2.1: A typical relay-assisted cooperative communication system

The notion of *user cooperation* was first introduced by Sendonaris *et al.* in [17] and analyzed in [18] as a new method for providing spatial diversity in wireless communication

systems. Meanwhile, Laneman *et al.* proposed several cooperative diversity protocols, based upon a two-phase transmission scheme where in the first phase, the source terminal broadcasts its data signal to all other terminals in the network. In the second phase, relay terminals retransmit their overheard information to the destination terminal. They have investigated the performance of the proposed cooperation protocols in terms of outage probability in [19]. In so-called *coded cooperation* [20, 21], Hunter *et al.* realize the concept of user cooperation through the distributed implementation of existing channel coding methods such as convolutional and turbo codes. The basic idea is that each user tries to transmit incremental redundancy for its partner. Their work can be considered as a systematic realization of selection relaying via powerful channel coding techniques.

Due to the interuser noisy channel and also the fact that each user needs to transmit its own information too, cooperative communications is not a simple relay problem [17]. For detailed analysis of cooperation communications, we refer the readers to [16, 17, 18, 19] and references therein.

In the following, we introduce some of the modes of operation and transmission protocols for processing the overheard information by the relay terminals commonly used in the analysis of cooperative communication networks.

2.4.1 Fixed Relaying

In fixed relaying, each relay may either amplify its received overheard signal subject to some power constraints, or may decode, re-encode, and retransmit it to the receiver [19].

Amplify-and-Forward (AaF)

In this mode, relay terminal amplifies the received overheard signal with respect to some power constraints and then forwards it to the receiver without demodulating or decoding the received signal. Use of channel state information (CSI) between the transmitter as the source and the relay terminal as the destination can determine the amplifying gain in the AaF mode. In one approach, also so-called CSI-based AaF relaying mode, relay terminal utilizes the instantaneous CSI of the source to relay link to scale its received data signal before retransmission. This ensures that the same output power is maintained for each realization. On the other hand, another approach is blind AaF scheme where there is no access to the CSI. In this mode, relay terminal simply employs some fixed power constraints.

This results in the preserved average output power, but allows for instantaneous output power to be larger than the average. Despite the better performance of CSI-based AaF mode, blind Aaf requires a much less complex relay terminal that makes it attractive from practical point of view.

In general, AaF scheme can be viewed as repetition coding from two separate transmitters, except that the relay terminal amplifies its own received noise as well.

Decode-and-Forward (DaF)

In this mode, the relay terminal decodes and re-encodes the received signal before retransmission. Decoding at the relay can take on a variety of forms. For example, the relay might fully decode, *i.e.*, estimate without error, the entire source codeword, or it might employ symbol-by-symbol decoding and allow the destination to perform full decoding. These options allow for trading off performance and complexity at the relay terminal [19]. It is also worth mentioning that in practice the AaF mode compared to the DaF mode requires significantly lower implementation complexity at the relay terminal [22]. In addition, the performance of DaF scheme is limited by the direct transmission between the source and relay terminal. However, it is shown by Yu *et al.* in [23] that in practice, the DaF mode slightly outperforms the AaF mode in terms of the average performance considering the possible unsuccessful cooperation scenarios in the $R \rightarrow D$ link.

2.4.2 Selection Relaying

In selection relaying, relay terminal forwards the received signal only if the instantaneous channel gain between the source and relay terminal is greater than a certain threshold. Otherwise, the source terminal simply continues its transmission to the destination terminal while the relay terminal remains silent [19].

2.4.3 Relay Transmission Protocols

In [22], Nabar *et al.* establish a unified framework of cooperation protocols for single-relay wireless networks. They quantify achievable performance gains for distributed schemes in an analogy to conventional co-located multi-antenna configurations. Specifically, they consider

three TDMA-based protocols named Protocol I, Protocol II, and Protocol III which correspond to traditional MIMO (multiple-input multiple-output), SIMO (single-input multiple-output) and MISO (multipe-input single-output) schemes, respectively. In the following, we describe these cooperation protocols which will be also a main focus of our work. Table 2.2 summarizes these protocols. Specifically, we have

Table 2.2: Cooperative protocols.

Time Slot\Protocol	I	II	III
1	$S \to R,\ D$	$S \to R,\ D$	$S \to R$
2	$S \to D,\ R \to D$	$R \to D$	$S \to D,\ R \to D$

Protocol I: The source terminal communicates with the relay and destination terminals during the first time slot. In the second time slot, both the relay and source terminals communicate with the destination terminal. This protocol realizes maximum degrees of broadcasting and receive collision.

Protocol II: In this protocol, the source terminal communicates with the relay and destination terminals over the first time slot. In the second time slot, only the relay terminal communicates with the destination terminal. This protocol realizes a maximum degree of broadcasting and exhibits no receive collision.

Protocol III: The third protocol is identical to Protocol I apart from the fact that the destination terminal remains silent during the first time slot. This protocol does not implement broadcasting but realizes receive collision.

Particularly, in Protocol II, the source terminal is silent over the second time slot, which implies that this protocol is more efficient than Protocols I and III in terms of battery life.

2.5 Cooperative Communications Channel Model

A cooperative communication system is composed of three nodes, i.e, a source terminal S, a relay terminal R and a destination terminal D. It is usually assumed that source to destination $S \to D$ link, source to relay $S \to R$ link and relay to destination $R \to D$ link undergo statistically independent fading. Figure 2.2 shows the schematic of such systems where h_{SD}, h_{SR} and h_{RD} are channel gains.

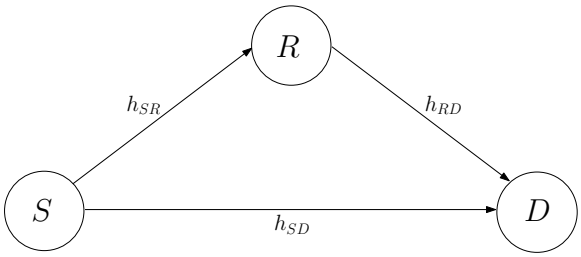

Figure 2.2: Cooperative communication system model

In this section, we introduce a widely used fading channel model, namely *Rayleigh fading channel*, as a framework that its knowledge is essential to the rest of this thesis in order to analyze the performance of cooperative communication systems. There are also other fading channel models used in the literature, see e.g. [24, 25, 26] and references therein.

2.5.1 Rayleigh Fading Channel

For a typical mobile wireless channel in urban areas, usually there is no line-of-sight component among cooperating nodes and consequently, the number of scatters is large. According to the Central Limit Theorem, the amplitude of the fading envelope follows a Rayleigh distribution, i.e., the magnitude of the channel gains, $|h_{SD}|$, $|h_{SR}|$ and $|h_{RD}|$, are Rayleigh random variables with the following distribution [27]:

$$f(x;\sigma) = \frac{x}{\sigma^2}\exp(\frac{-x^2}{2\sigma^2}), \qquad \text{for } x \geq 0. \tag{2.8}$$

In this thesis, we assume that the channel is time-varying but frequency-flat fading and adopt the user cooperation protocol III mentioned in section 2.4.3. For the $R \rightarrow D$ link, the AaF mode is used. It should be noted that channel gains h_{SD}, h_{SR} and h_{RD} are zero-mean complex Gaussian random variables with variance $\frac{\sigma^2}{2}$ per dimension, denoted by $\mathcal{CN} \sim (0, \sigma^2)$.

Let two consecutive signals transmitted by the source terminal, using BPSK modulation, be denoted as x_1 and x_2. In the first signaling interval, the signal received at the relay terminal is given as

$$r_R = \sqrt{E_{SR}}h_{SR}x_1 + n_R, \tag{2.9}$$

where E_{SR} is the average energy available at the relay terminal considering different path loss and possible shadowing effects in the $S \rightarrow R$ link. h_{SR} is distributed as $\mathcal{CN} \sim (0, \sigma^2_{SR})$

over $S \to R$ link with variance $\sigma_{SR}^2/2$ per dimension. The noise term n_R is assumed to be $\mathcal{CN} \sim (0, N_0)$ with variance $N_0/2$ per dimension.

The relay terminal scales the received signal r_R by a factor of $\eta = 1/\sqrt{\mathrm{E}\{|r_R|^2\}}$ to ensure the average energy unity and retransmits the signal during the second time slot. The received signal at the destination terminal in the second time slot is

$$r = \sqrt{E_{RD}} h_{RD} \frac{r_R}{\sqrt{\mathcal{E}\{|r_R|^2\}}} + \sqrt{E_{SD}} h_{SD} x_2 + n_D, \tag{2.10}$$

where n_D is the additive noise term modelled as $\mathcal{CN} \sim (0, N_0)$ with variance $N_0/2$ per dimension. E_{SD} and E_{RD} represent the average energies available at the destination terminal. h_{SD} and h_{RD} are complex Gaussian fading channel gains over $S \to D$ and $R \to D$ links with variance $\sigma_{SD}^2/2$ and $\sigma_{RD}^2/2$ per dimension, respectively.

Substituting (2.9) and $\mathrm{E}\{|r_R|^2\} = E_{SR} + N_0$ into (2.10), we have

$$r = \sqrt{\frac{E_{RD} E_{SR}}{E_{SR} + N_0}} h_{RD} h_{SR} x_1 + \sqrt{E_{SD}} h_{SD} x_2 + \tilde{n}, \tag{2.11}$$

where $\tilde{n} = \sqrt{\frac{E_{RD}}{E_{SR}+N_0}} h_{RD} n_R + n_D$.

Now, conditioned on h_{RD}, the effective noise term is found to be complex Gaussian with zero mean and variance

$$\mathrm{E}\{|\tilde{n}|^2\} = N_0 \left(1 + \frac{E_{RD}|h_{RD}|^2}{E_{SR} + N_0}\right). \tag{2.12}$$

Assuming that the destination terminal normalizes the received signal in (2.11) by a factor of $\sqrt{1 + E_{RD}|h_{RD}|^2/(E_{SR} + N_0)}$ [22], the received signal at the destination terminal after the second time interval is as follows

$$r = \alpha h_{SR} h_{RD} x_1 + \beta h_{SD} x_2 + n, \tag{2.13}$$

where, conditioned on h_{RD}, the noise term n is $\mathcal{CN} \sim (0, N_0)$ random variable with variance $N_0/2$ per dimension and α and β are normalization factors due to the AaF mode given by [28]

$$\begin{aligned} \alpha &= \sqrt{\frac{(E_{SR}/N_0)E_{RD}}{1 + E_{SR}/N_0 + |h_{RD}|^2 E_{RD}/N_0}}, \\ \beta &= \sqrt{\frac{(1 + E_{SR}/N_0)E_{SD}}{1 + E_{SR}/N_0 + |h_{RD}|^2 E_{RD}/N_0}}. \end{aligned} \tag{2.14}$$

2.5.2 Imperfect Channel State Information

The significant performance difference between coherent and non-coherent combining suggests the importance of channel knowledge in wireless wideband systems [5]. Typically, most of researchers assume perfect channel knowledge when they analyze the performance of a cooperative communication system. However, in practice, channel gains need to be estimated and then used in the detection process. Channel estimation can be done via pilot-based scheme or a decision-feedback scheme [5]. For more detailed information on channel estimation the readers can refer to [4, 5], and references therein.

Typically, channel estimation is not error free. Therefore, in this section, we present a general framework to model the estimation error used in the rest of this thesis.

We can model the estimation error as follows [29]

$$\hat{h} = h + e, \tag{2.15}$$

where h is the channel gain and its estimate denoted by $\hat{h}$. The error term e is a zero-mean complex Gaussian random variable with variance σ_e^2. Therefore, $\hat{h}$ is a zero-mean complex Gaussian random variable with variance $\sigma_{\hat{h}}^2 = \sigma_h^2 + \sigma_e^2$. The correlation coefficient of h and $\hat{h}$ is given by $\rho_{h\hat{h}} = \frac{\mathcal{E}[h\hat{h}^*]}{2\sigma_h\sigma_{\hat{h}}}$. Since h and $\hat{h}$ are jointly Gaussian, conditioned on $\hat{h}$, we can rewrite h as

$$h = \rho\hat{h} + d, \tag{2.16}$$

where

$$\rho = \rho_{h\hat{h}}\sigma_{\hat{h}}/\sigma_h = \frac{\sigma_{\hat{h}}^2}{\sigma_{\hat{h}}^2 + \sigma_e^2}, \tag{2.17}$$

and d is a zero-mean complex Gaussian random variable with variance

$$\sigma_d^2 = (1 - \rho_{h\hat{h}}^2)\sigma_{\hat{h}}^2 = \frac{\sigma_{\hat{h}}^2\sigma_e^2}{\sigma_{\hat{h}}^2 + \sigma_e^2}. \tag{2.18}$$

2.6 Summary

This chapter reviewed fundamental concepts of wireless cooperative communication systems. It surveyed different diversity combining techniques, protocols for cooperative diversity and presented a channel model framework, knowledge of which is essential to the rest of this thesis.

Chapter 3

PSAM In Cooperative Networks

Pilot symbol assisted modulation (PSAM) scheme is used to estimate the channel gains based on the minimum-mean-squared-error (MMSE) criterion by periodically inserting pilot symbols known to a receiver into the data sequence. References [30, 31, 32], and [33] provide a detailed description of PSAM.

In this chapter, we analyze the performance of PSAM scheme in a relay-assisted network that operates in the AaF mode. We derive the correlation coefficients of the fading channel gains and their estimates for both fading and non-fading $R \to D$ link. We show that the presence of fading in the $R \to D$ link manifests itself with the introduction of additional Doppler frequency terms. We further derive a closed form expression for the BEP in terms of Doppler frequency, number of pilot symbols and SNR.

3.1 System Model

The cooperative communication system shown in Figure 2.2 is considered. We assume a time-varying frequency-flat Rayleigh fading channel and adopt the user cooperation protocol III discussed in Section 2.4.3 with the AaF protocol.

Denoting the two consecutive signals transmitted by the source terminal using BPSK modulation as x_1 and x_2, the received signal at the destination terminal after the second time slot is given by

$$r = \alpha h_{SR} h_{RD} x_1 + \beta h_{SD} x_2 + n, \tag{3.1}$$

where h_{SD}, h_{SR} and h_{RD} are the complex Gaussian channel gains over $S \to D$, $S \to R$

and $R \rightarrow D$ links with variance $\sigma_{SD}^2/2$, $\sigma_{SR}^2/2$ and $\sigma_{RD}^2/2$ per dimension, respectively. Conditioned on h_{RD}, the noise term n is a zero-mean complex Gaussian random variable with variance $N_0/2$ per dimension. α and β are given by (2.14).

We now employ STBC due to their inherent orthogonal structure, an essential feature for channel estimation and data detection. For the case of single relay terminal, we need to use STBC designed for two transmit antennas, i.e., the Alamouti scheme introduced in Section 2.3.2. For this purpose, the two data signals x_1 and x_2 are simultaneously sent during four consecutive signaling time slots.

The corresponding detected signals at the destination terminal can then be written as

$$\hat{x}_1 = \alpha \hat{h}_{SR}^* \hat{h}_{RD}^* r_1 + \beta \hat{h}_{SD} r_2^*, \tag{3.2}$$

$$\hat{x}_2 = -\alpha \hat{h}_{SR} \hat{h}_{RD} r_2^* + \beta \hat{h}_{SD}^* r_1, \tag{3.3}$$

where r_1 and r_2 are received signals at the destination terminal D after the second and the forth time slots, respectively, and are given by

$$r_1 = \alpha h_{SR} h_{RD} x_1 + \beta h_{SD} x_2 + n_1, \tag{3.4}$$

$$r_2 = -\alpha h_{SR} h_{RD} x_2^* + \beta h_{SD} x_1^* + n_2. \tag{3.5}$$

3.2 PSAM for distributed STBC

In the considered PSAM scenario, each frame consists of 2 pilot symbols, P_1 and P_2, and $M-2$ data symbols as shown in Figure 3.1. We assume that each frame consists of $\frac{M}{2}$ sub blocks each of which comprising two symbols. Under the assumption of non-fading $R \rightarrow D$ link, i.e., $h_{RD} = 1$, and that the channel gains remain constant over four symbol intervals, the received signals at the k^{th} $(0 \leq k < \frac{M}{2})$ sub block in the j^{th} frame can be obtained from (3.4) and (3.5) as

$$\begin{aligned} r_1^{k,j} &= \alpha h_{SR}^{k,j} x_1^{k,j} + \beta h_{SD}^{k,j} x_2^{k,j} + n_1^{k,j}, \\ r_2^{k,j} &= -\alpha h_{SR}^{k,j} x_2^{k,j} + \beta h_{SD}^{k,j} x_1 + n_2^{k,j}. \end{aligned} \tag{3.6}$$

Assuming, without loss of generality, that pilot symbols $(P_1 = 1, P_2 = 1)$ are positioned at the beginning of each frame, i.e., sub-block $k = 0$, we can write the received pilot signals at the destination terminal as

$$\begin{aligned} r_1^{0,j} &= \alpha h_{SR}^{0,j} x_1^{0,j} + \beta h_{SD}^{k,j} x_2^{0,j} + n_1^{0,j} \\ r_2^{0,j} &= -\alpha h_{SR}^{0,j} x_2^{0,j} + \beta h_{SD}^{0,j} x_1 + n_2^{0,j}. \end{aligned} \tag{3.7}$$

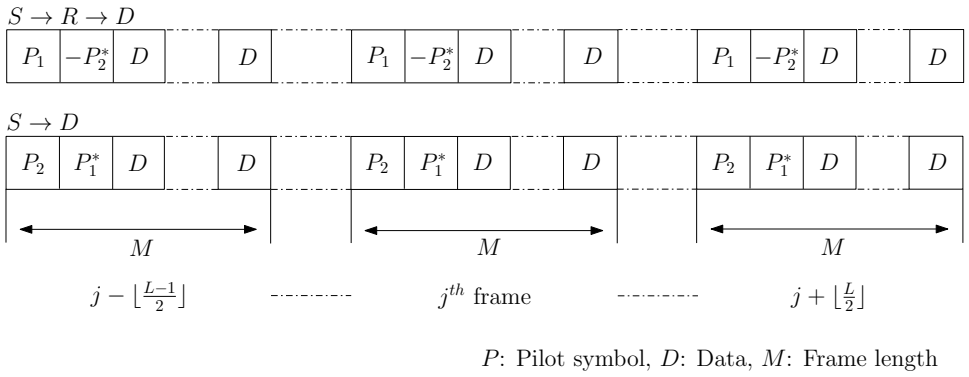

Figure 3.1: Frame structure for pilot-symbol-assisted channel estimation.

Based on the received signals corresponding to pilot symbol transmissions, the destination terminal employs a Wiener filter to estimate the fading coefficients [30].

As depicted in Fig. 3.1, we assume that $\lfloor L/2 \rfloor$ pilot symbols from the following frames, $\lfloor (L-1)/2 \rfloor$ pilot symbols from the previous frames and one current frame are employed in the estimation. The estimate of fading channel gains for the $S \to R \to D$ and $S \to D$ links at the k^{th} sub block in the j^{th} frame are obtained, respectively, as

$$\hat{h}_{SR}^{k,j} = \sum_{j=-\lfloor (L-1)/2 \rfloor}^{\lfloor L/2 \rfloor} w_j^k \left(\alpha h_{SR}^{0,j} + \frac{n_1^{0,j} - n_2^{0,j}}{2} \right), \tag{3.8}$$

$$\hat{h}_{SD}^{k,j} = \sum_{j=-\lfloor (L-1)/2 \rfloor}^{\lfloor L/2 \rfloor} w_j^k \left(\beta h_{SD}^{0,j} + \frac{n_1^{0,j} + n_2^{0,j}}{2} \right), \tag{3.9}$$

where w_j^k's are the interpolation coefficients in the j^{th} frame. It is worth mentioning that the estimated value in (3.8) is the same for the same sub block in different frames whereas it is different for different sub blocks in a single frame. Therefore, the index j in $\hat{h}_{SR}^{k,j}$ can be dropped for brevity. The same also applies to $\hat{h}_{SD}^{k,j}$ in (3.9).

The variance of $\hat{h}_{SR}^{k,j}$ is given by

$$\begin{aligned} \sigma^2_{\hat{h}_{SR}^{k,j}} &= \frac{\alpha^2}{2} \sum_{i=-\lfloor \frac{(L-1)}{2} \rfloor}^{\lfloor L/2 \rfloor} \sum_{j=-\lfloor \frac{(L-1)}{2} \rfloor}^{\lfloor L/2 \rfloor} w_i^k (w_j^k)^* \mathrm{E}\left[h_{SR}^{0,i} (h_{SR}^{0,j})^* \right] \\ &+ \frac{N_0}{4} \sum_{j=-\lfloor \frac{(L-1)}{2} \rfloor}^{\lfloor L/2 \rfloor} |w_j^k|^2. \end{aligned} \tag{3.10}$$

Considering Bessel-type autocorrelation function

$$\mathrm{E}\left[h_{SR}^{0,i}(h_{SR}^{0,j})^*\right] = 2\sigma_{SR}^2 J_0(2\pi f T_{SR}|i-j|M), \tag{3.11}$$

where $J_0(.)$ is the zero-order Bessel function of the first kind and fT_{SR} is the normalized Doppler frequency for $S \to R$ link, we have

$$\begin{aligned} r_{h_{SR}\hat{h}_{SR}}^{k,j} &= \frac{1}{2}\mathrm{E}\left[h_{SR}^{k,j}(\hat{h}_{SR}^{k,j})^*\right] \\ &= \alpha \sum_{j=-\lfloor\frac{(L-1)}{2}\rfloor}^{\lfloor L/2\rfloor} (w_j^k)\sigma_{SR}^2 J_0(2\pi f T_{SR}|2k-j|M). \end{aligned} \tag{3.12}$$

Following [34], the correlation coefficient of the squared amplitude of the fading estimates for $S \to R \to D$ link with the underlying non-fading $R \to D$ link, $\rho_{S\to R\to D}^s$, is given by [35]

$$\begin{aligned} \rho_{S\to R\to D}^s &= \frac{\left(r_{h_{SR}\hat{h}_{SR}}^{k,j}\right)^2}{\sigma_{h_{SR}^{k,j}}^2 \sigma_{\hat{h}_{SR}^{k,j}}^2} \\ &= \frac{\left(\sum_j (w_j^k)^* J_0(2\pi f T_{SR}|2k-j|M)\right)^2}{\sum_i \sum_j w_i^k (w_j^k)^* J_0(2\pi f T_{SR}|i-j|M) + \frac{N_0}{4\sigma_{SR}^2\alpha^2}\sum_j |w_j^k|^2}. \end{aligned} \tag{3.13}$$

For the asymptotic case of $E_{SD}/N_0 = E_{RD}/N_0 \gg 1$ with perfect power control and sufficiently large $E_{SR}/N_0 > E_{SD}/N_0$, the normalization coefficients in (2.14) reduce to $\alpha = \beta = \sqrt{E_{SD}}$. Then, the correlation coefficient in (3.13) becomes a function of Doppler value, the SNR and the number of interpolation coefficients.

Similarly, it can be shown that the correlation coefficient for $S \to D$ link, $\rho_{S\to D}^s$, is given by [35]

$$\rho_{S\to D}^s = \frac{\left(\sum_j (w_j^k)^* J_0(2\pi f T_{SD}|2k-j|M)\right)^2}{\sum_i \sum_j w_i^k (w_j^k)^* J_0(2\pi f T_{SD}|i-j|M) + \frac{1}{4\sigma_{SR}^2\alpha^2}\sum_j |w_j^k|^2}. \tag{3.14}$$

where fT_{SD} is the normalized Doppler frequency for $S \to D$ link.

When the underlying $R \to D$ link is subject to fading, we can write the j^{th} fading estimate for $S \to R \to D$ link as

$$\hat{h}_{SR}^{k,j}\hat{h}_{RD}^{k,j} = \sum_{j=-\lfloor\frac{(L-1)}{2}\rfloor}^{\lfloor L/2\rfloor} w_j^k \left(\alpha h_{SR}^{0,j} h_{RD}^{0,j} + \frac{n_1^{0,j} - n_2^{0,j}}{2}\right). \tag{3.15}$$

Following similar steps used in the derivation of (3.13), we can find the *fading* correlation coefficient, $\rho^f_{S\to R\to D}$, as [35]

$$\rho^f_{S\to R\to D} = \frac{\left(\sum_j (w_j^k)^* J_0(2\pi f T_{SR}|2k-j|M) J_0(2\pi f T_{RD}|2k-j|M)\right)^2}{\sum_i \sum_j w_i^k (w_j^k)^* J_0(2\pi f T_{SR}|i-j|M) J_0(2\pi f T_{RD}|i-j|M) + \frac{N_0}{4\sigma^2_{SR}\sigma^2_{RD}E_{SD}} \sum_j |w_j^k|^2}. \tag{3.16}$$

Here, fT_{RD} is the normalized Doppler frequency for the fading $R \to D$ link. It can be observed from comparison of (3.13) and (3.16) that the presence of fading in the $R \to D$ link manifests itself with the introduction of an additional Doppler frequency term. In other words, the time-varying nature of $R \to D$ link will increase the *effective* Doppler speed observed by the destination terminal. It should also be noted that (3.13) and (3.16) are the same when h_{RD} is non-fading, i.e. $fT_{RD} = 0$[1]. In addition, due to the embedded orthogonality, $\rho^f_{S\to D}$ under the effect of fading $R \to D$ link is still equal to its static counterpart $\rho^s_{S\to D}$ given by (3.14).

3.3 Bit Error Probability

In this section, we present detailed derivation of the bit error probability (BEP) expression for the aforementioned system model. We adopt BPSK modulation where $x_1 = x_2$ or $x_1 = -x_2$, each with probability $\frac{1}{2}$. According to the BPSK decision rule, if $\mathrm{Re}[\hat{x}_i] > 0$ $(i = 1, 2)$, then $\hat{x}_i$ is demodulated to 1, otherwise $\hat{x}_i = -1$ is chosen. Without loss of generality, we consider the detection of $\hat{x}_1$, noting that the same steps can be followed in the detection of the symbol $\hat{x}_2$.

Since h_{SR} and $\hat{h}_{SR}$ are jointly Gaussian, we can write the channel gain h_{SR} in terms of its estimate $\hat{h}_{SR}$ using (2.16). As a result, conditioned on $\hat{h}_{SR}$, the channel gain can be written as

$$h_{SR} = \rho_{SR}\hat{h}_{SR} + d_{SR}, \tag{3.17}$$

where ρ_{SR} is given by (2.17) and d_{SR} is a $\mathcal{CN} \sim (0, \sigma^2_{d_{SR}})$ random variable where its variance is given by (2.18). Similarly, we can write h_{SD} and h_{RD} in terms of their estimates. Assuming that all links experience identical statistics, we have $\rho_{SD} = \rho_{SR} = \rho_{RD} = \rho$ and $\sigma^2_{d_{SD}} = \sigma^2_{d_{SR}} = \sigma^2_{d_{RD}} = \sigma^2_d$.

[1]Note that $\alpha^2 = E_{SD}$ and $\sigma^2_{RD} = 1$

For the case of $x_1 = x_2$, assuming that the receiver estimates h_{RD} correctly, and substituting (3.4) and (3.5) into (3.2), we obtain

$$\begin{aligned}\hat{x}_1 &= \rho x_1 \left[\alpha^2|h_{RD}|^2|\hat{h}_{SR}|^2 + \beta^2|\hat{h}_{SD}|^2 + \alpha\beta\hat{h}_{SD}\left((\hat{h}_{SR}h_{RD})^* - \hat{h}_{SR}h_{RD}\right)\right] \\ &+ x_1\left[\alpha^2|h_{RD}|^2\hat{h}^*_{SR} + \beta^2\hat{h}_{SD}d^*_{SD} + \alpha\beta\left((\hat{h}_{SR}h_{RD})^*d_{SD} - \hat{h}_{SD}h_{RD}d_{SR}\right)\right] \\ &+ \alpha\hat{h}^*_{SR}h^*_{RD}n_1 + \beta\hat{h}_{SD}n^*_2. \end{aligned} \tag{3.18}$$

The assumption of correctly estimated h_{RD} is realistic, since the SNR over the $R \to D$ link is typically much higher than that over other links. If otherwise is assumed, the mathematical analysis will become highly complicated.

Now, conditioned on $\hat{h}_{SR}$ and $\hat{h}_{SD}$, $\mathrm{Re}\{\hat{x}_1\}$ is

$$\mathrm{Re}\{\hat{x}_1\} = Cx_1 + \psi, \tag{3.19}$$

where ψ is a zero-mean Gaussian random variable with variance

$$\sigma^2_\psi = \sigma^2_d\left(\beta^2 + \alpha^2|h_{RD}|^2 + \frac{N_0}{2}\right)\left(\alpha^2|h_{RD}|^2|\hat{h}_{SR}|^2 + \beta^2|\hat{h}_{SD}|^2\right), \tag{3.20}$$

and the coefficient C is given by

$$C = \rho\left(\alpha^2|h_{RD}|^2|\hat{h}_{SR}|^2 + \beta^2|\hat{h}_{SD}|^2\right). \tag{3.21}$$

Therefor, noting that the average bit error probability is, in general, given by $\overline{P}_e = Q(\sqrt{\mathrm{SNR}})$, it can be shown that

$$P^{h_{RD},\hat{h}_{SD},\hat{h}_{SR}}_{e|x_1=+x_2} = Q\left(\sqrt{\frac{\rho^2\left(\alpha^2|h_{RD}|^2|\hat{h}_{SR}|^2 + \beta^2|\hat{h}_{SD}|^2\right)}{\sigma^2_d\left(\beta^2 + \alpha^2|h_{RD}|^2 + \frac{N_0}{2}\right)}}\right). \tag{3.22}$$

Since $\Pr\{x_1 = +x_2\} = \Pr\{x_1 = -x_2\} = \frac{1}{2}$, thus $P^{h_{RD},\hat{h}_{SD},\hat{h}_{SR}}_{e|x_1=+x_2} = P^{h_{RD},\hat{h}_{SD},\hat{h}_{SR}}_{e|x_1=-x_2}$. Therefore the BEP, conditioned on h_{RD}, $\hat{h}_{SD}$ and $\hat{h}_{SR}$, is still given by (3.22). We also recall from (2.17) that $\sqrt{\rho}$ is the correlation coefficient of the channel gains and their estimates.

Subsequently, assuming $E_{SD}/N_0 = E_{RD}/N_0 \gg 1$ and for sufficiently large $E_{SR}/N_0 > E_{SD}/N_0$, the normalization factors α and β reduce to $\sqrt{E_{SD}}$. Thus, we can rewrite (3.22) in terms of the channel correlation coefficient $\rho^f_{S\to R\to D}$ and the end-to-end instantaneous SNR, γ, as follows

$$P_{e|h_{RD},\hat{h}_{SR},\hat{h}_{SD}} = Q\left(\sqrt{\frac{2\gamma\rho(|h_{RD}|^2|\hat{h}_{SR}|^2 + |\hat{h}_{SD}|^2)}{(1+|h_{RD}|^2)(1+(1-\rho)\gamma)}}\right), \tag{3.23}$$

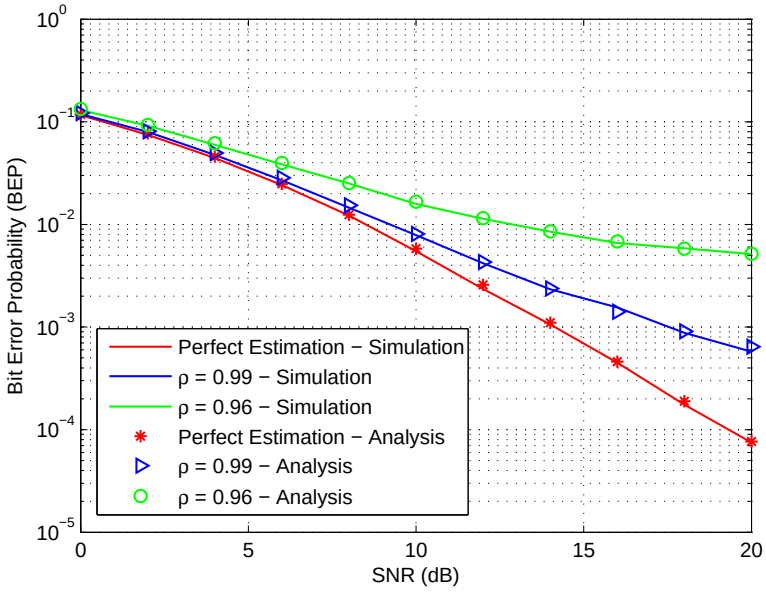

Figure 3.2: BEP with respect to various values of ρ for non-fading $R \to D$ link.

where $\rho = \rho^f_{S\to R\to D}$ given by (3.16) when the underlying $R \to D$ link is subject to fading, and

$$\gamma = \frac{\sigma^2_{SR} E_{SD}}{N_0}(1 + |h_{RD}|^2). \tag{3.24}$$

After some mathematical manipulations, presented in the Appendix A, we obtain [36]

$$P_e = \frac{1}{\pi}\int_0^{\pi/2} \left(\frac{\sin^2\theta}{\sin^2\theta + \bar{\zeta}_1}\right)\left(\frac{\sin^2\theta}{\sin^2\theta + \bar{\zeta}_2}\right) d\theta, \tag{3.25}$$

where

$$\bar{\zeta}_1 = \frac{\gamma\rho|h_{RD}|^2}{(1 + |h_{RD}|^2)(1 + (1-\rho)\gamma)}, \tag{3.26}$$

$$\bar{\zeta}_2 = \frac{\gamma\rho}{(1 + |h_{RD}|^2)(1 + (1-\rho)\gamma)}. \tag{3.27}$$

Therefore, the BEP is a function of channels correlation coefficient expressed in (3.16), which is a function of Doppler frequency, SNR and the number of pilot symbols in a PSAM-assisted STBC network.

For the non-fading $R \to D$ link, i.e. $h_{RD} = 1$, the BEP expression in (3.25) is reduced

to [36]

$$P_e^{h_{RD}=1} = \frac{1}{4}\left(1 - \sqrt{\frac{\bar{\zeta}}{2+\bar{\zeta}}}\right)^2 \left(2 + \sqrt{\frac{\bar{\zeta}}{2+\bar{\zeta}}}\right), \tag{3.28}$$

where $\bar{\zeta}$ is calculated by substituting $h_{RD} = 1$ in either (3.26) or (3.27).

3.4 Numerical Results

In this section, numerical results for the analytical observations in the previous section are presented. In this simulation study, we consider BPSK modulation and assume $E_{SD} = E_{RD}$, i.e., $S \to D$ and $R \to D$ links are balanced, which can be achieved through power control. As for the $S \to R$ link, we set $E_{SR}/N_0 = 30$dB. First, we assume a non-fading $R \to D$ link. Figure 3.2 depicts BEP versus SNR with respect to various values for correlation coefficients $\rho^f_{S\to R\to D}$. In this case, there is a perfect match between the analytical expressions and simulation results. On the other hand, when fading $R \to D$ link is considered in the system model, the analytical expression for BEP in (3.25) becomes a lower bound. For lower-range SNR's it nearly matches the simulation results. However, as the value of SNR increases, it gradually diverges from simulation at higher-range SNR's for about 1 dB.

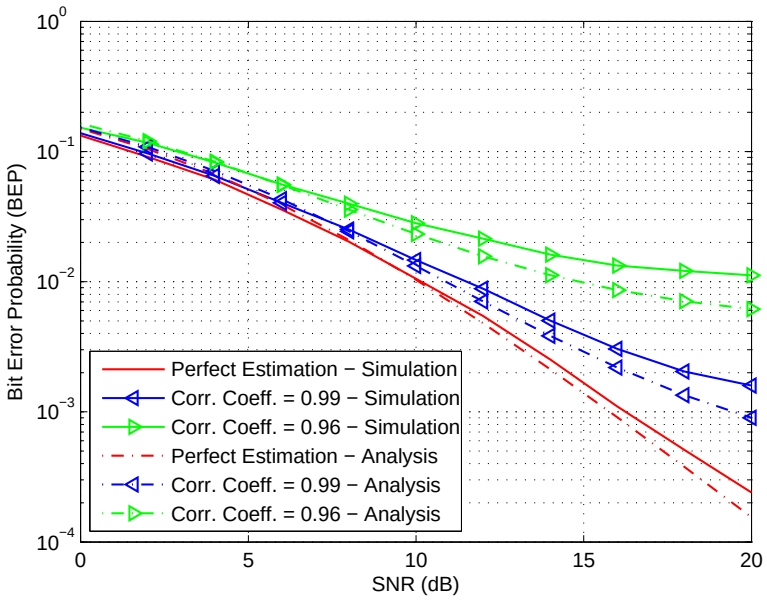

Figure 3.3: BEP with respect to various values of ρ for fading $R \to D$ link.

3.5 Summary

This chapter investigated the impact of imperfect channel estimation on the performance of PSAM for a distributed STBC system operating in AaF relaying mode. We concluded that the time varying nature of $R \rightarrow D$ link increases the effective Doppler speed observed by the destination terminal. This would bring about more errors in the estimation. However, with the relation of the correlation coefficients and the number of pilot symbols derived in this chapter, one can optimally choose the number of pilots in order to compensate for the estimation error when the fading and Doppler effects are severe. Moreover, an analytical expression for the BEP was also presented, which turned out to be a function of Doppler frequency, number of pilot symbols and the end-to-end instantaneous SNR.

Chapter 4

Multi-Relay Two-Way Cooperative Networks

In most practical scenarios, the data transmission in cooperative communication networks occurs via a half-duplex *one-way* channel that results in the bandwidth loss. To overcome this problem, bidirectional or *two-way* relaying has recently been proposed [37, 38]. Subsequently, many researchers have focused on these two-way channels [39, 40]. In particular, some of them have investigated the performance of these systems in terms of outage probability, see e.g. [40, 41].

There are also a number of works on the relay selection (RS) in two-way relay-assisted networks. In [39], Hwang *et al.* consider two-way AaF relaying communication over a multiple-relay cooperative network in which the best relay terminal is selected based on the instantaneous channel information. In [42], Ju *et al.* propose a joint RS-OSS[1] protocol to maximize the mutual information between the two end-source terminals. The same authors propose a relay selection scheme based on the max-min criterion in [41] to minimize the outage probability. However, in their works they assume that all the channel gains are known to the both end-sources and the relays. In fact, many of the current results on selection cooperation are built upon the assumption that there is perfect channel state information at every terminal [39, 40].

As previously discussed, channel coefficients must be estimated in practice. Specifically, due to imperfect CSI, performance of the system is confined to a specific bound where the

[1] opportunistic source selection

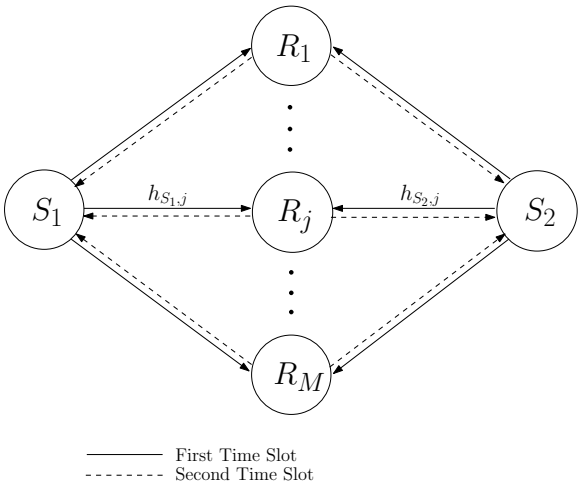

Figure 4.1: Two-way cooperative communication system model with multiple relays.

system can not surpass it. In other words, the outage probability of the system has an error floor.

This chapter aims to investigate the performance of max-min relay selection in the two-way multi-relay cooperative networks with imperfect CSI.

4.1 System model

A two-way relay-assisted wireless communication system, also known as *two-way channel*, is considered where two end-source terminals, S_1 and S_2, communicate with assistance of multiple relay terminals, R_j for $j = 1, ..., M$, as shown in Figure 4.1. Each terminal is equipped with a single antenna and operates in a half-duplex mode. The AaF relaying mode is adopted where the exchange of information takes place in two different time slots. At the first time slot, the selected best relay terminal R_{j^*} receives the sum signal from S_1 and S_2. In the second time slot, the relay terminal amplifies and forwards the received signal to both end-source terminals S_1 and S_2. We assume that non of the terminals has the perfect knowledge of the channel gains and thus has to estimate the channel coefficients with some errors. Considering time-varying frequency-flat Rayleigh fading reciprocal channels, every channel gain is modelled as a complex Gaussian random variable $h_{S_i,j} \sim \mathcal{CN}(0, \sigma^2_{S_i})$ with variance $\sigma^2_{S_i}$ per dimension.

Now let the two data signals transmitted at the first time slot by two end-source terminals

be denoted as x_1 and x_2, respectively. The received sum signal at the relay terminal R_j is given by

$$r_j = \sqrt{E_{S_1}} h_{S_1,j} x_1 + \sqrt{E_{S_2}} h_{S_2,j} x_2 + n_j, \tag{4.1}$$

where E_{S_1} and E_{S_2} are the transmit powers at S_1 and S_2, respectively, and n_j is the AWGN noise modelled as a $\mathcal{CN}(0, \sigma_{n_j}^2)$ with variance $\sigma_{n_j}^2$ per dimension.

At the second time slot, the relay terminal R_j amplifies the receive signal r_j with an amplifying coefficient η and then broadcasts it to S_1 and S_2 over the two-way broadcast channel. The received signal at S_i, denoted by y_i, is as follows

$$y_i = \sqrt{E_R} \eta h_{S_i,j} r_j + n_{S_i}, \tag{4.2}$$

where n_{S_i} is also the AWGN noise modelled as a complex $\mathcal{CN}(0, \sigma_{n_{S_i}}^2)$ with variance $\sigma_{n_{S_i}}^2$ per dimension.

To ensure that the transmission power at the relay terminal is confined to E_R, η should be determined as

$$\begin{aligned} \eta &= \frac{1}{\sqrt{E_{S_1}|h_{S_1,j}|^2 + E_{S_2}|h_{S_2,j}|^2 + \sigma_{n_j}^2}} \\ &\cong \frac{1}{\sqrt{E_{S_1}|h_{S_1,j}|^2 + E_{S_2}|h_{S_2,j}|^2}}. \end{aligned} \tag{4.3}$$

The approximation in (4.3) is to simplify the analytical derivations. Section 4.5 verifies through the numerical results that the effect of such approximation is quite negligible.

Substituting (4.1) into (4.2) and cancelling the self-interference of the end-source terminal S_i, i.e., $\sqrt{E_{S_i} E_R} \eta h_{S_i,j}^2 x_i$ for $i = 1, 2$, we obtain[2]

$$y_1 = \sqrt{E_{S_2} E_R} \eta h_{S_1,j} h_{S_2,j} x_2 + \sqrt{E_R} \eta h_{S_1,j} n_j + n_{S_1}, \tag{4.4}$$

$$y_2 = \sqrt{E_{S_1} E_R} \eta h_{S_1,j} h_{S_2,j} x_1 + \sqrt{E_R} \eta h_{S_2,j} n_j + n_{S_2}. \tag{4.5}$$

One can assume that the end-source terminal S_i cancels out its self-interference with imperfect CSI, i.e., cancelling $\sqrt{E_{S_i} E_R} \eta \hat{h}_{S_i,j}^2 x_i$ instead of $\sqrt{E_{S_i} E_R} \eta h_{S_i,j}^2 x_i$. In this case, the system performance degrades due to the self-interference error terms in the received signal

[2]We note that each end-source terminal knows its own symbol x_i and so it can simply remove this term from the received signal.

y_i at S_i. In Section 4.5, we have demonstrated this effect in Figure 4.4. However, in the rest of this thesis we assume perfect self-interference cancellation.

In order to detect the transmitted data signals at each S_i from the received signal y_i, we have to use the estimated channel coefficients due to the imperfect CSI at every terminal. So, we have

$$\hat{x}_2 = \hat{h}^*_{S_1,j}\hat{h}^*_{S_2,j}y_1, \quad \hat{x}_1 = \hat{h}^*_{S_1,j}\hat{h}^*_{S_2,j}y_2, \tag{4.6}$$

where $\hat{x}_2$ and $\hat{x}_1$ are the detected signals at $\mathcal{S}_1$ and S_2, respectively, and $\hat{h}_{S_i,j}$ is the estimation of $h_{S_i,j}$, distributed as $\mathcal{CN}(0, \frac{\sigma^2_{S_i}}{\rho_{S_i}})$ and related to $h_{S_i,j}$ by [29]

$$h_{S_i,j} = \rho_{S_i}\hat{h}_{S_i,j} + d_{S_i}, \tag{4.7}$$

where $\sqrt{\rho_{S_i}}$ is the correlation coefficient between the actual channel gain $h_{S_i,j}$ and its estimate $\hat{h}_{S_i,j}$ calculated from (2.17), and d_{S_i} is a zero-mean complex Gaussian random variable with variance given by (2.18).

To find the end-to-end instantaneous SNR's $\gamma_{S_1,j}$ and $\gamma_{S_2,j}$ for the links $S_1 \to R_j \to S_2$, and $S_2 \to R_j \to S_1$, respectively, first we need to detect the signals at two end-sources. Without loss of generality, we consider detecting of $\hat{x}_2$ at S_1. Therefore, we obtain:

$$\hat{x}_2 = \sqrt{E_{S_2}E_R}\eta\rho_{S_1}\rho_{S_2}|\hat{h}_{S_1,j}|^2|\hat{h}_{S_2,j}|^2x_2 + \psi + \varrho, \tag{4.8}$$

where ψ is the noise term and ϱ is the error term due to the estimation errors and are as follow

$$\psi = \hat{h}^*_{S_1,j}\hat{h}^*_{S_2,j}n_{S_1} + \sqrt{E_R}\eta n_j\left(\rho_{S_1}|\hat{h}_{S_1,j}|^2\hat{h}^*_{S_2,j} + \hat{h}^*_{S_1,j}\hat{h}^*_{S_2,j}d_{S_1}\right), \tag{4.9}$$

$$\varrho = \sqrt{E_{S_2}E_R}\eta x_2\left(\rho_{S_1}|\hat{h}_{S_1,j}|^2\hat{h}^*_{S_2,j}d_{S_2} + \rho_{S_2}|\hat{h}_{S_2,j}|^2\hat{h}^*_{S_1,j}d_{S_1} + \hat{h}^*_{S_1,j}\hat{h}^*_{S_2,j}d_{S_1}d_{S_2}\right) \tag{4.10}$$

We also have a similar expression for $\hat{x}_1$.

The instantaneous SNR, $\gamma_{S_2,j}$ can then be calculated as [43]

$$\gamma_{S_2,j} = \frac{E_{S_2}E_R\rho^2_{S_1}\rho^2_{S_2}|\hat{h}_{S_1,j}|^2|\hat{h}_{S_2,j}|^2}{\alpha_2|\hat{h}_{S_1,j}|^2 + \beta_2|\hat{h}_{S_2,j}|^2 + C_2}, \tag{4.11}$$

Similarly, we have

$$\gamma_{S_1,j} = \frac{E_{S_1}E_R\rho^2_{S_1}\rho^2_{S_2}|\hat{h}_{S_1,j}|^2|\hat{h}_{S_2,j}|^2}{\beta_1|\hat{h}_{S_1,j}|^2 + \alpha_1|\hat{h}_{S_2,j}|^2 + C_1}, \tag{4.12}$$

where

$$\begin{cases} \alpha_2 = E_R\rho_{S_1}^2(E_{S_2}\sigma_{d_{S_2}}^2 + \sigma_{n_j}^2) + E_{S_2}\sigma_{n_{S_1}}^2, \\ \beta_2 = E_{S_2}(E_R\rho_{S_2}^2\sigma_{d_{S_1}}^2 + \sigma_{n_{S_1}}^2), \\ C_2 = \alpha_2\left(\frac{\sigma_{d_{S_1}}^2}{\rho_{S_1}^2}\right), \end{cases} \tag{4.13}$$

and

$$\begin{cases} \alpha_1 = E_R\rho_{S_2}^2(E_{S_1}\sigma_{d_{S_1}}^2 + \sigma_{n_j}^2) + E_{S_1}\sigma_{n_{S_2}}^2, \\ \beta_1 = E_{S_1}(E_R\rho_{S_1}^2\sigma_{d_{S_2}}^2 + \sigma_{n_{S_2}}^2), \\ C_1 = \alpha_1\left(\frac{\sigma_{d_{S_2}}^2}{\rho_{S_2}^2}\right). \end{cases} \tag{4.14}$$

It should be noted that since the relay R_j dose not have the knowledge of the actual channel coefficients $h_{S_i,j}$'s, the estimated values, $\hat{h}_{S_i,j}$'s, should be used in (4.3) as well.

In section 4.3 we use $\gamma_{S_i,j}$ to derive the outage probability of the system where we assume that C_i is small enough and therefore we ignore the effect of C_i in the denominator. We show through the simulations that this assumption is realistic and the analytical results are accurate.

It is worth mentioning that, assuming each terminal has perfect CSI *i.e.* $\rho_{S_i} = 1$ and $\sigma_{d_{S_i}}^2 = 0$, and for the unit-variance noise signals, $\gamma_{S_2,j}$ reduces to

$$\gamma_{S_{2,j}} = \frac{E_S E_R|\hat{h}_{S_1,j}|^2|\hat{h}_{S_2,j}|^2}{(E_S + E_R)|\hat{h}_{S_1,j}|^2 + E_S|\hat{h}_{S_2,j}|^2}, \tag{4.15}$$

which has a similar form to the result reported earlier in [41]. The same also holds true for $\gamma_{S_1,j}$.

4.2 Relay Selection with Imperfect CSI

The max-min relay selection scheme where the best relay is the one that maximizes the minimum received SNR at the two end-source terminals is considered in this section. In other words, the best relay terminal, R_{j^*}, maximizes the minimum of received end-to-end SNR's $\gamma_{S_1,j}$ and $\gamma_{S_2,j}$ over all relay terminals R_j's, where

$$j^* = \arg\max_{j=1,\ldots,M} \min\{\gamma_{S_1,j}, \gamma_{S_2,j}\}, \tag{4.16}$$

In this thesis, we consider outage probability as the probability that either or both of the users are in outage,[3] i.e,

$$P_{\text{out}} = \Pr[\min\{\gamma_{S_1,j}, \gamma_{S_2,j}\} < \gamma_{th}]. \tag{4.17}$$

Taking into the account the relay selection scheme, we can compute P_{out} as

$$P_{\text{out}} = \Pr[\min\{\gamma_{S_1,j^*}, \gamma_{S_2,j^*}\} < \gamma_{th}], \tag{4.18}$$

where $\gamma_{th} = 2^R - 1$ for some total network rate R.

4.3 Outage Probability

In this section, we investigate the effect of imperfect CSI on the performance of the two-way relay-assisted networks described in section 4.1 in terms of the outage probability.

In order to find a closed-form expression for P_{out}, we need to derive the CDF, $F_X(x)$, of $X = \max_{j=1,\ldots,M}\{X_j\}$, where $X_j = \min\{\gamma_{S_1,j}, \gamma_{S_2,j}\}$. Then, the outage probability is given by

$$P_{\text{out}} = F_X(\gamma_{th}). \tag{4.19}$$

We first derive the CDF of X_j, presented in the Appendix B, as

$$F_{X_j}(x) = F^1_{X_j}(x) + F^2_{X_j}(x), \tag{4.20}$$

where $F^1_{X_j}(x)$ is given by [43]

$$\begin{aligned} F^1_{X_j}(x) &= \frac{\rho_{S_1}}{\rho_{S_1}+\rho_{S_2}} + \frac{\rho_{S_2}}{\rho_{S_1}+\rho_{S_2}} \exp\left(\frac{-x}{K_1}(\alpha_1+\beta_1)(\rho_{S_1}+\rho_{S_2})\right) \\ &- A\left[\frac{2x}{K_1}\sqrt{\alpha_1\beta_1\rho_{S_1}\rho_{S_2}}\mathcal{K}_1\left(\frac{2x}{K_1}\sqrt{\alpha_1\beta_1\rho_{S_1}\rho_{S_2}}\right)\right. \\ &- \left.\sum_{i=0}^{\infty}\frac{(-1)^i}{i!}\left(\frac{x}{K_1}\alpha_1\rho_{S_2}\right)^{(i+1)} E_{i+2}\left(\frac{x}{K_1}\beta_1\rho_{S_1}\right)\right]. \end{aligned} \tag{4.21}$$

where $K_1 = E_{S_1}E_R\rho^2_{S_1}\rho^2_{S_2}$, $A = \exp\left[\frac{-x}{K_1}(\alpha_1\rho_{S_1} + \beta_1\rho_{S_2})\right]$, $\mathcal{K}_1(.)$ is the modified Bessel function of the second kind with order 1, and $E_i(.)$ is the exponential integral function

[3] Another scenario could be to consider that the system is in outage if all the users are in outage. In this case if any user can transmit its signal to its destination successfully, then the system would not be in outage.

defined in Eq. (5.4.1) of [44]. $F^2_{X_j}(x)$ is also simply derived by substituting ρ_{S_1}, α_1, β_1 and K_1 by ρ_{S_2}, α_2, β_2 and K_2, respectively. Finally, the CDF of X is given by

$$F_X(x) = \prod_{j=1}^{M} F_{X_j}(x). \tag{4.22}$$

$F_X(x)$ is a function of α_i, β_i and K_i that all are functions of the correlation coefficients ρ_{S_1} and ρ_{S_2}. Therefore, the channel estimation error degrades the performance of the system and can dramatically change the outage probability of a two-way relay-assisted network. In Section 4.5, we demonstrate the effect of channel estimation errors in all links on the system's performance through changing ρ_{S_1} and ρ_{S_2}.

It should be noted that in order to have the outage probability when the perfect CSI is present to all the terminals, one needs to simply substitute $\rho_{S_i} = 1$ and $\sigma^2_{d_{S_i}} = 0$ into (4.21).

4.4 Power Allocation Scheme

In this section, we investigate an optimum power allocation scheme for the mentioned two-way relay networks. For this purpose, we note that if ρ_{S_1} and ρ_{S_2} in $F^1_{X_j}(x)$ and $F^2_{X_j}(x)$ are replaced with their average $\frac{\rho_{S_1}+\rho_{S_2}}{2}$, $F_{X_j}(x)$ remains almost the same (see Appendix C for proof).

In other words, this observation states that the outage probability is in practice a function of the average estimation errors modelled by the correlation coefficients ρ_{S_1} and ρ_{S_2} and hence neither of the links $S_1 \to R_j \to S_2$ and $S_2 \to R_j \to S_1$ dominates the performance of the system. In section 4.5, Monte Carlo simulations also confirms these observations.

The problem of power allocation optimization can be stated as

$$\begin{aligned} &\{E^{opt}_{S_1}, E^{opt}_{S_2}\} = \arg \min_{E_{S_1}, E_{S_2}} \{p_{out}\} \\ &\text{subject to} \qquad E_{S_1} + E_{S_2} = E, \end{aligned} \tag{4.23}$$

where E is the total transmission power for the two links.

It should be noted here that, minimizing the p_{out} is equivalent to maximizing $\gamma_{S_1,j}$ and $\gamma_{S_2,j}$. Therefore, rewriting $\gamma_{S_1,j}$ and $\gamma_{S_2,j}$ in terms of E_{S_1} and E_{S_2} and replacing ρ_{S_1} and ρ_{S_2} with their average, we have

$$\gamma_{S_1,j} = \frac{E_R \rho^4 |\hat{h}_{S_1,j}|^2 |\hat{h}_{S_2,j}|^2 E_{S_1}}{B E_{S_1} + E_R \sigma^2_{n_j} (\rho^2 |\hat{h}_{S_2,j}|^2 + \sigma^2_{d_S})}, \tag{4.24}$$

where

$$B = (E_R \rho^2 \sigma_{d_S}^2 + \sigma_{n_{S_2}}^2) \left(|\hat{h}_{S_1,j}|^2 + |\hat{h}_{S_2,j}|^2 + \frac{\sigma_{d_S}^2}{\rho^2} \right), \tag{4.25}$$

$\rho = \frac{\rho_{S_1} + \rho_{S_2}}{2}$, and $\sigma_{d_{S_1}} = \sigma_{d_{S_2}} = \sigma_{d_S}$.

We note that $\gamma_{S_1,j}$ in (4.24) is a monotonically increasing function of E_{S_1}. Similarly, $\gamma_{S_2,j}$ is a monotonically increasing function of E_{S_2}. Next, we note that $E_{S_1} + E_{S_2} = E$ is fixed, and also the effect of ρ_{S_1} and ρ_{S_2} on both $\gamma_{S_1,j}$ and $\gamma_{S_2,j}$ is only specified by their average. Therefore, in order to maximize the minimum of $\gamma_{S_1,j}$ and $\gamma_{S_2,j}$ or equivalently to minimize the p_{out}, the optimum power allocation is $E_{S_1} = E_{S_2} = \frac{E}{2}$ [43]. In other words, to guarantee the highest probability . that neither of the links are in outage, we have to allocate the same transmission power to both end-source terminals regardless of the estimation error in each link. However, if our goal is that at least one of the links survives the outage, we have to allocate the transmission power E_{S_i} proportional to the ρ_{S_i}.

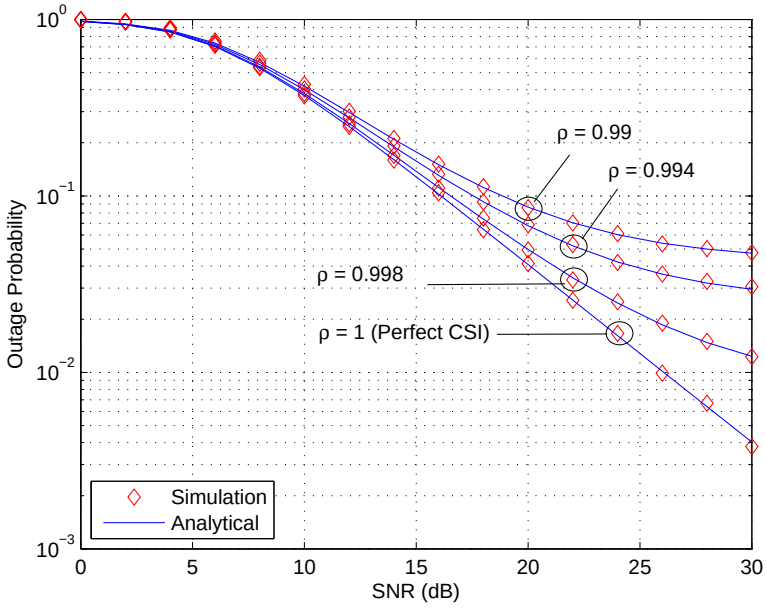

Figure 4.2: Outage probability for various values of ρ, for a single-relay network.

4.5 Numerical Results

In our simulation study, we assume unit-variance noise at the relay terminal after the first time slot, i.e., $\sigma_{n_j}^2 = 1$ for all relays. First, we consider $\rho_{S_1} = \rho_{S_2} = \rho$. Figure 4.2 shows the outage probability versus SNR with respect to various values for correlation coefficient ρ in a single relay scenario. It is evident form Figure 4.2 that in two-way networks, there is an error floor due to the presence of estimation error. In other words, since increasing SNR does not lead to a decrease in the P_{out}, there is no diversity gain for such networks in the presence of estimation error. It is worth mentioning that despite ignoring the effect of C_i's

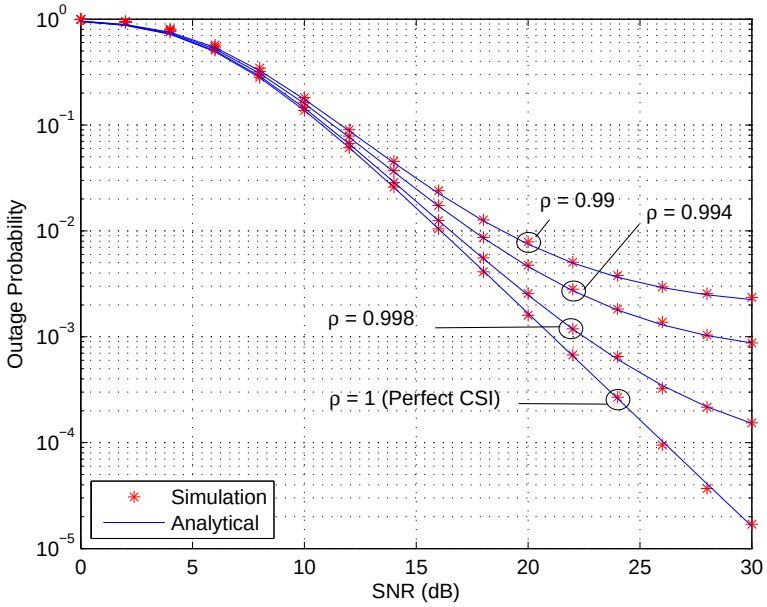

Figure 4.3: Outage probability for various values of ρ, for $M = 2$ relay terminals.

in the denominator of $\gamma_{S_1,j}$ and $\gamma_{S_2,j}$ in (4.11) and (4.12) and using the approximation in (4.3), there is a perfect match between our analytical results and simulations.

Figure 4.3 depicts outage probability versus SNR with respect to various values for correlation coefficients ρ with $M = 2$ relay terminals. It confirms that increasing the number of relay terminals leads to lower outage probability.

In Figure 4.4, we have shown the impact of imperfect self-interference cancellation on the performance of multi-relay two-way networks. It compares the performance of perfect and imperfect self-interference cancellation for $M = 2$ relay terminals. There is about 5dB

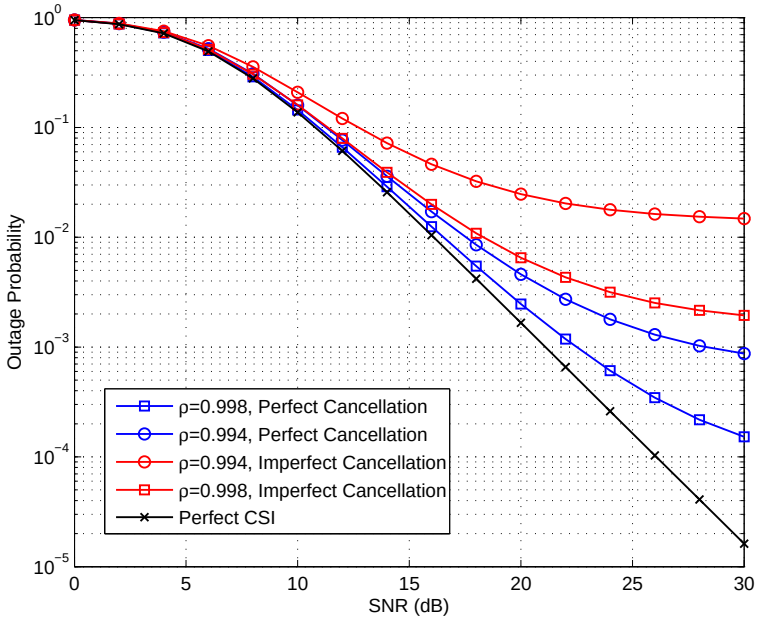

Figure 4.4: Performance comparison of perfect and imperfect self-interference cancellation at the end-source terminals for $M = 2$ relay terminals.

degradation in SNR due to the self-interference error terms in the received signals.

In Figure 4.5, we have compared the performance of a two-way network with $M = 1, 2, 3,$ and 4 different relay terminals for the fixed value of $\rho = 0.995$ in order to better show the effect of the number of relays on P_{out}. For example, there is about 10dB improvement in SNR in a network with $M = 4$ relay terminals compared to the single-relay network.

As discussed in section 4.4, the performance of a two-way cooperative network in terms of outage probability is dominated by neither of the $S_1 \rightarrow R_j \rightarrow S_2$ or $S_2 \rightarrow R_j \rightarrow S_1$ links. Instead, it is determined by the average performance of both links. Figure 4.6 depicts the outage probability for different ρ_{S_1}, ρ_{S_2} and $\rho = \frac{\rho_{S_1}+\rho_{S_2}}{2}$. It clearly corroborates the analytical results in section 4.4. For example, for $\rho_{S_1} = 0.98$ and $\rho_{S_2} = 1$, P_{out} is the same as $\rho_{S_1} = \rho_{S_2} = \rho = 0.99$. Analytical expressions in (4.19) and (4.21), when ρ_{S_1} and ρ_{S_2} are replaced with their average, perfectly match with the simulation results and are omitted here for the sake of illustration.

Figure 4.7 shows the effect of proposed power allocation scheme on the P_{out} for $\rho = 0.98$ and $\rho = 0.95$. There is a slight improvement when $E_{S_1} = E_{S_2}$ compared to when

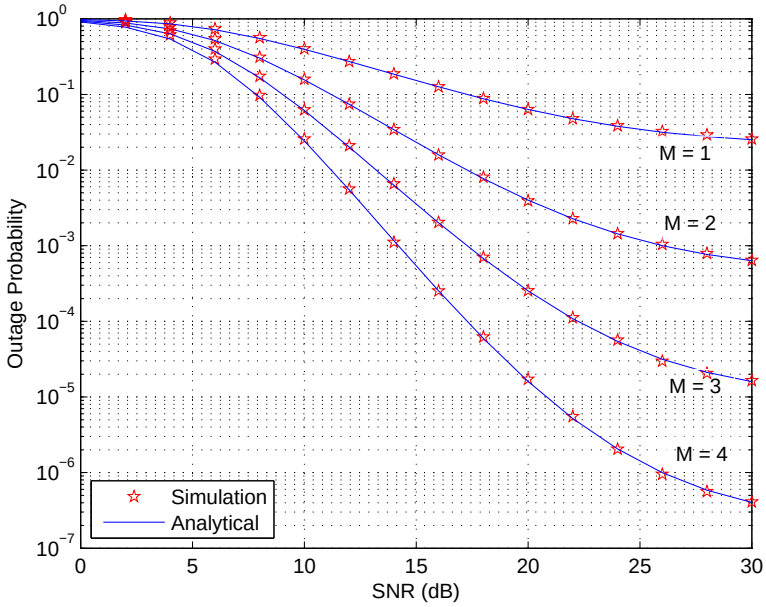

Figure 4.5: Performance comparison of a two-way network with $M = 1, 2, 3,$ and 4 relay terminals for $\rho = 0.995$.

$E_{S_1} = 2 \times E_{S_2}$. However, there is 1dB improvement when $E_{S_1} = E_{S_2}$ compared to when $E_{S_1} = 4 \times E_{S_2}$. As the gap between E_{S_1} and E_{S_2} increases, the performance of the system degrades. For higher SNR's, however, the graphs for all allocated power values experience the error floor.

4.6 Summary

In this chapter, we analyzed the effect of estimation error on the performance of the two-way cooperative networks. First, we derived a closed form expression for the CDF of the end-to-end SNR which we subsequently used to find the the outage probability of the system when the best relay is selected. We demonstrated that the presence of estimation error leads to a loss in diversity gain or equivalently an error floor.

In addition, we proved that neither of the links $S_1 \rightarrow R_j \rightarrow S_2$ and $S_2 \rightarrow R_j \rightarrow S_1$ dominates the performance of the system. We further presented an optimum power allocation scheme that minimizes the P_{out}.

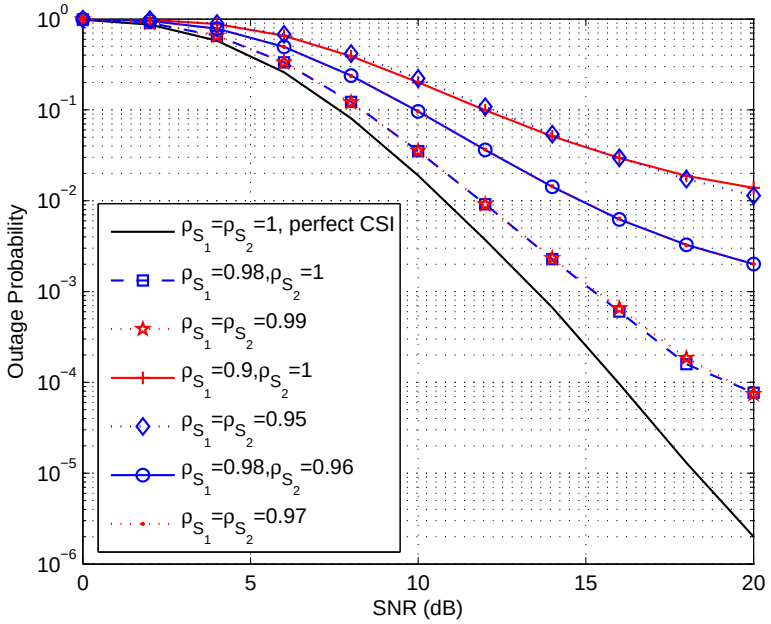

Figure 4.6: Outage probability for various values of ρ_{S_1} and ρ_{S_2} for $M = 4$ relay terminals.

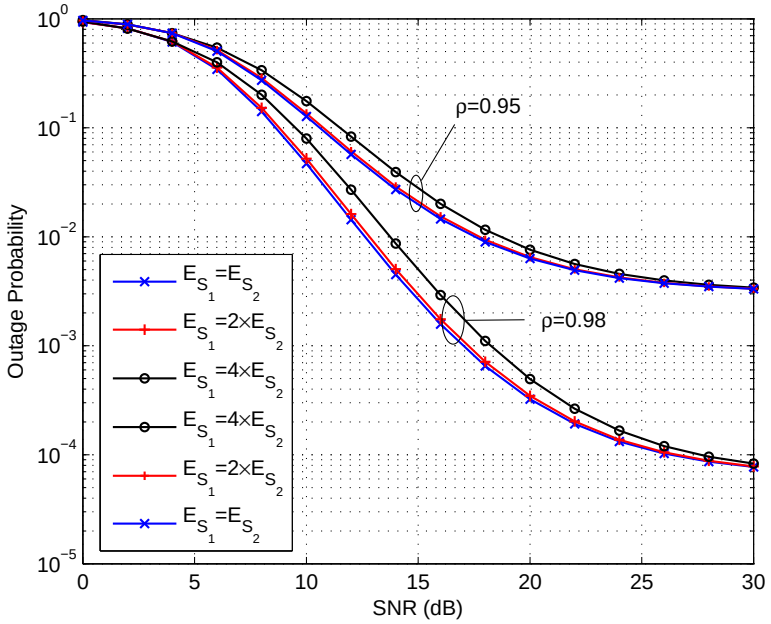

Figure 4.7: The proposed power allocation scheme for $\rho = 0.98$ and $\rho = 0.95$ and for $M = 4$ relay terminals. There is about 1dB improvement in the SNR.

Chapter 5

Conclusion And Future Work

This final chapter summarizes the contributions of the work presented in this thesis and suggests several directions for further research.

5.1 Conclusion

Cooperative networks have recently attracted much attention and fundamental information-theoretic aspects of these networks have been already well documented. However, practical implementation of cooperative communications requires an in-depth investigation of several physical layer issues such as channel estimation.

In this thesis, we have first investigated the performance of cooperative communication systems with imperfect channel estimation in chapter 3, where the channel estimates are obtained through the use of pilot symbols. We have presented an exact bit error probability expression in the presence of channel estimation errors which is in terms of the correlation coefficient of the fading channel gains and their estimates. We have derived the relation between the number of pilot symbols and the bit error probability of the system.

We have also studied the effect of imperfect channel estimation in two-way multi-relay cooperative networks. In our model, we have adopted the max-min relay selection algorithm. We have derived an exact expression for the CDF of the instantaneous end-to-end SNR of the system based on which the outage probability has been presented in chapter 4. We have further shown that neither of the $S_1 \rightarrow R \rightarrow S_2$ and $S_2 \rightarrow R \rightarrow S_1$ links dominates the performance of the system in a two-way setup scenario and have accordingly proposed a novel optimum power allocation scheme to minimize the outage probability.

5.2 Future Work

An initial problem for future consideration is generalizing our framework for analyzing the effect of imperfect CSI on the performance of cooperative communications systems to other wireless channel models. We elaborate some of these extensions in the following.

- **PSAM scheme in cascaded Rayleigh fading environment:** The first extension to the results of chapter 3 is to derive the correlation coefficient for the *cascaded* or *Double Rayleigh* fading channels where each channel gain is a product of two independent Gaussian random variables. Moreover, having known the relation of the bit error probability and the number of pilot symbols from chapter 3, an interesting problem is to find the optimum number of pilot symbols to minimize the error probability subject to some power constraint in the training phase.

- **BEP of two-way multi-relay networks with imperfect CSI:** To find the bit error probability of a two-way multi-relay network with imperfect CSI, we first need to find the statistical characteristics of the system such as PDF and MGF of the instantaneous end-to-end SNR. Having the CDF presented in chapter 4, it is straight forward to derive these statistical tools. For instance, substituting the CDF into the relation $P_e = \frac{a}{\sqrt{2\pi}} \int_0^\infty F_\gamma \left(\frac{t^2}{b}\right) \exp\left(\frac{-t^2}{2}\right) dt$ presented in [45], we can find the BEP of the system.

- **Two-way relaying networks with outdated CSI:** The outdated feedback of CSI can dramatically degrade the efficiency of diversity in cooperative networks leading to crushing the diversity gain. Consequently, the study of such effects seems essential. The general framework of this scenario is similar to the one presented in chapter 4. The effect of feedback delay has been well studied in one-way cooperative networks, see e.g. [46, 47]. However, it is yet have to be considered for the two-way networks.

Appendix A

MGF Approach To BER

In section 3.3, we derived the bit error probability as

$$P_e = \mathrm{E}\left\{ Q\left(\sqrt{2\left(\overline{\zeta}_1 |\hat{h}_{SR}|^2 + \overline{\zeta}_2 |\hat{h}_{SD}|^2 \right)} \right) \right\}, \tag{A.1}$$

where $\bar{\zeta}_1$ and $\bar{\zeta}_2$, conditioned on h_{RD}, are deterministic and given by (3.26) and (3.27). Therefore, $X_1 = \bar{\zeta}_1 |\hat{h}_{SR}|^2$ and $X_2 = \bar{\zeta}_2 |\hat{h}_{SD}|^2$ are exponential random variables. To further simplify (A.1) we exploit the moment generating function (MGF) of X_1 and X_2 given by $M_{X_i}(-s) = \int_0^\infty \exp(-sX_i) f_{X_i}(x_i) dx_i$.

Using the alternative representation of the Q-function, given by

$$Q(x) = \frac{1}{\pi} \int_0^{\frac{\pi}{2}} \exp\left(\frac{-x^2}{2\sin^2\theta} d\theta \right), \tag{A.2}$$

we can rewrite (A.1) as

$$\begin{aligned} P(e) &= \frac{1}{\pi} \times \int_0^{\pi/2} \int_0^\infty \int_0^\infty \exp\left(-s(X_1 + X_2)\right) f_{X_1}(x_1) f_{X_2}(x_2) dx_1 dx_2 d\theta \\ &= \frac{1}{\pi} \int_0^{\pi/2} M_{X_1}(-s) M_{X_2}(-s) d\theta, \end{aligned} \tag{A.3}$$

where $s = \frac{1}{\sin^2\theta}$ and the MGF of the exponential random variables X_i is given by $M_{X_i}(s) = \frac{1}{1-\bar{\zeta}_i s}$. Therefore,

$$P(e) = \frac{1}{\pi} \int_0^{\pi/2} \left(\frac{\sin^2\theta}{\sin^2\theta + \overline{\zeta}_1} \right) \left(\frac{\sin^2\theta}{\sin^2\theta + \overline{\zeta}_2} \right) d\theta. \tag{A.4}$$

Appendix B

Derivation Of $F_{X_j}(x)$

In this appendix, we present the derivation of $F_{X_j}(x)$ in more details. According to the definition of a cumulative distribution function, $F_{X_j}(x) = \Pr\{\min\{\gamma_{S_1,j}, \gamma_{S_2,j}\} \leq x\}$. We can rewrite it as $F_{X_j}(x) = F^1_{X_j}(x) + F^2_{X_j}(x)$, where

$$F^1_{X_j}(x) = \Pr\{\gamma_{S_1,j} \leq x, |\hat{h}_{S_1,j}|^2 < |\hat{h}_{S_2,j}|^2\}, \tag{B.1}$$

$$F^2_{X_j}(x) = \Pr\{\gamma_{S_2,j} \leq x, |\hat{h}_{S_1,j}|^2 \geq |\hat{h}_{S_2,j}|^2\}. \tag{B.2}$$

Substituting (4.12) into (B.1), we have

$$F^1_{X_j}(x) = \Pr\left\{(K_1|\hat{h}_{S_2,j}|^2 - \beta_1 x)|\hat{h}_{S_1,j}|^2 \leq \alpha_1|\hat{h}_{S_2,j}|^2 x, |\hat{h}_{S_1,j}|^2 < |\hat{h}_{S_2,j}|^2\right\}. \tag{B.3}$$

Now following a similar approach as in [41], we can rewrite it as

$$\begin{aligned} F^1_{X_j}(x) &= \Pr\left\{|\hat{h}_{S_1,j}|^2 < |\hat{h}_{S_2,j}|^2, |\hat{h}_{S_2,j}|^2 \leq \frac{(\alpha_1+\beta_1)x}{K_1}\right\} \\ &+ \Pr\left\{|\hat{h}_{S_1,j}|^2 < \frac{\alpha_1|\hat{h}_{S_2,j}|^2 x}{K_1|\hat{h}_{S_2,j}|^2 - \beta_1 x}, |\hat{h}_{S_2,j}|^2 > \frac{(\alpha_1+\beta_1)x}{K_1}\right\}. \end{aligned} \tag{B.4}$$

Therefore, it can be calculated as follows

$$\begin{aligned} F^1_{X_j}(x) &= \underbrace{\int_0^\infty f_2(t)dt - \int_0^{\frac{(\alpha_1+\beta_1)x}{K_1}} [1 - F_1(t)]f_2(t)dt}_{I_1} \\ &- \underbrace{\int_{\frac{(\alpha_1+\beta_1)x}{K_1}}^\infty \left[1 - F_1(\frac{\alpha x t}{K_1 t - \beta_1 x})\right] f_2(t)dt}_{I_2}, \end{aligned} \tag{B.5}$$

where $f_2(t)$ is the PDf of $|\hat{h}_{S_2,j}|^2$ and $F_1(t)$ is the CDf of $|\hat{h}_{S_1,j}|^2$. Since $|\hat{h}_{S_1,j}|^2$ and $|\hat{h}_{S_2,j}|^2$ are exponentially distributed with parameters ρ_{S_1} and ρ_{S_2}, respectively, we can simplify I_1 as

$$I_1 = \frac{1}{\rho_{S_1}+\rho_{S_2}}\left[\rho_{S_1}+\rho_{S_2}e^{\left(-\frac{x}{K_1}(\alpha_1+\beta_1)(\rho_{S_1}+\rho_{S_2})\right)}\right], \tag{B.6}$$

and by using the substitution $y = t - \frac{\beta_1 x}{K_1}$ we have

$$\begin{aligned} I_2 &= A\rho_{S_2}\int_{\frac{\alpha_1 x}{K_1}}^{\infty}\exp\left[-\frac{\alpha_1\beta_1\rho_{S_1}x^2}{K_1^2 y}-\rho_{S_2}y\right]dy \\ &= A\rho_{S_2}\left[\int_0^{\infty}\exp\left[-\frac{\alpha_1\beta_1\rho_{S_1}x^2}{K_1^2 y}-\rho_{S_2}y\right]dy-\int_0^{\frac{\alpha_1 x}{K_1}}\exp\left[-\frac{\alpha_1\beta_1\rho_{S_1}x^2}{K_1^2 y}-\rho_{S_2}y\right]dy\right]. \end{aligned} \tag{B.7}$$

where $A = \exp\left[\frac{-x}{K_1}(\alpha_1\rho_{S_1}+\beta_1\rho_{S_2})\right]$. We can further simplify it by using Eq. (3.471.9) of [48] and Taylor series for the exponential function as follows

$$\begin{aligned} I_2 &= \frac{2Ax}{K_1}\sqrt{\alpha_1\beta_1\rho_{S_1}\rho_{S_2}}\mathcal{K}_1\left(\frac{2x}{K_1}\sqrt{\alpha_1\beta_1\rho_{S_1}\rho_{S_2}}\right) \\ &- A\sum_{i=0}^{\infty}\frac{(-1)^i}{i!}\left(\frac{x}{K_1}\alpha_1\rho_{S_2}\right)^{(i+1)}E_{i+2}\left(\frac{x}{K_1}\beta_1\rho_{S_1}\right), \end{aligned} \tag{B.8}$$

where $E_{i+2}(x) = \int_0^1 t^i e^{-\frac{x}{t}}dt$ is the exponential integral function defined in Eq. (5.4.1) of [44]. Now, plugging (B.6) and (B.8) into (B.5) results in (4.21). Following similar steps, we can also derive $F^2_{X_j}(x)$.

Appendix C

Effect Of The $\frac{\rho_{S_1}+\rho_{S_2}}{2}$ On The P_{out}

In this appendix, we discuss the results presented in section 4.4 analytically and draw a proof that if ρ_{S_1} and ρ_{S_2} in $F^1_{X_j}(x)$ and $F^2_{X_j}(x)$ are replaced with their average $\frac{\rho_{S_1}+\rho_{S_2}}{2}$, $F_{X_j}(x)$ remains almost the same. Therefore, the outage probability is determined by the average of estimation error.

To prove it mathematically, we perform the mentioned substitution and use the approximation $(\rho_{S_1}+\rho_{S_2})^2 \approx 4\rho_{S_1}\rho_{S_2}$ which holds accurate enough for $0 \leq \rho_{S_1}, \rho_{S_2} \leq 1$. We first note that the terms $\sqrt{\alpha_1\beta_1\rho_{S_1}\rho_{S_2}}\mathcal{K}_1\left(\frac{2x}{K_1}\sqrt{\alpha_1\beta_1\rho_{S_1}\rho_{S_2}}\right)$ and $\exp\left(\frac{-x}{K_1}(\alpha_1+\beta_1)(\rho_{S_1}+\rho_{S_2})\right)$ remain exactly the same after replacing ρ_{S_1} and ρ_{S_2} with their average. By performing the substitution in the summation term on the right hand side of (4.21) and considering the same approximation, we obtain the ith term of the summation as

$$\begin{aligned}&\frac{(-1)^i}{i!}\left(\frac{x}{K_1}\alpha_1(\frac{\rho_{S_1}+\rho_{S_2}}{2})\right)^{(i+1)} E_{i+2}\left(\frac{x}{K_1}\beta_1(\frac{\rho_{S_1}+\rho_{S_2}}{2})\right)\\ &\quad=\frac{(-1)^i}{i!}\left(\frac{x}{K_1}\alpha_1\sqrt{\rho_{S_1}\rho_{S_2}}\right)^{(i+1)} E_{i+2}\left(\frac{x}{K_1}\beta_1\sqrt{\rho_{S_1}\rho_{S_2}}\right)\end{aligned} \tag{C.1}$$

Therefore, we need to verify that

$$\begin{aligned}&\frac{(-1)^i}{i!}\left(\frac{x}{K_1}\alpha_1\rho_{S_2}\right)^{(i+1)} E_{i+2}\left(\frac{x}{K_1}\beta_1\rho_{S_1}\right) \approx\\ &\frac{(-1)^i}{i!}\left(\frac{x}{K_1}\alpha_1\sqrt{\rho_{S_1}\rho_{S_2}}\right)^{(i+1)} E_{i+2}\left(\frac{x}{K_1}\beta_1\sqrt{\rho_{S_1}\rho_{S_2}}\right).\end{aligned} \tag{C.2}$$

For this purpose we define an error term ξ_1 to be the difference of the left-hand side and the right-hand side terms in (C.2). Without loss of generality, we assume that $\rho_{S_2} > \rho_{S_1}$

and that $\rho_{S_2} = \rho_{S_1} + \epsilon$ for $0 < \epsilon < 1$ [1].Therefore,

$$\xi_1 = O\left(\int_0^1 t^i e^{-\frac{\beta_1 x \rho_{S_1}}{K_1 t}}(1 - e^{-\frac{\beta_1 x \epsilon}{K_1 t}})dt\right), \tag{C.3}$$

similarly, for the term A we find the error term ξ_2 as follows

$$\xi_2 = O\left(\sqrt{\exp\{-\frac{x\epsilon}{E_R \rho_{S_1}^2(\rho_{S_1}+\epsilon)^2}\}}\right). \tag{C.4}$$

Therefore, the final error in F_{X_j} after replacing ρ_{S_i}'s with their average, is of the order $2\xi_1\xi_2$. Comparing this error to the rest of the terms in $F_{X_j}(x)$ numerically shows that this error is negligible. Therefore, the value of $F_X(x)$ remains almost the same.

[1]For the ordinary case that $\epsilon = 0$, i.e, $\rho_{S_1} = \rho_{S_2}$, the proof is straight forward.

Bibliography

[1] S. Hui and K. Yeung, "Challenges in the migration to 4G mobile systems," *IEEE Commun. Magazine*, vol. 41, no. 12, pp. 54–59, 2003.

[2] B. Rankov and A. Wittneben, "Spectral efficient protocols for half-duplex fading relay channels," *IEEE J. Sel. Areas Commun.*, vol. 25, no. 2, pp. 379–389, 2007.

[3] T. Koike-Akino, P. Popovski, and V. Tarokh, "Optimized constellations for two-way wireless relaying with physical network coding," *IEEE J. Sel. Areas Commun.*, vol. 27, no. 5, pp. 773–787, 2009.

[4] C. Patel and G. Stuber, "Channel estimation for amplify and forward relay based cooperation diversity systems," *IEEE Trans. Wireless Commun.*, vol. 6, no. 6, pp. 2348–2356, 2007.

[5] D. Tse and P. Viswanath, *Fundamentals Of Wireless Communication.* Cambridge Univ. Pr., 2005.

[6] A. Sheikh, *Wireless Communications: Theory And Techniques.* Kluwer Academic Pub., 2004.

[7] A. Nosratinia, T. Hunter, and A. Hedayat, "Cooperative communication in wireless networks," *IEEE Commun. Magazine*, vol. 42, no. 10, pp. 74–80, Oct. 2004.

[8] A. Wittneben, "Basestation modulation diversity for digital SIMULCAST," in *Proc. 41st IEEE VTC*, 2002, pp. 848–853.

[9] ——, "A new bandwidth efficient transmit antenna modulation diversity scheme for linear digital modulation," in *Proc. IEEE ICC*, vol. 3, 2002, pp. 1630–1634.

[10] N. Seshadri and J. Winters, "Two signaling schemes for improving the error performance of FDD transmission systems using transmitter antenna diversity," in *Proc. 43rd IEEE VTC*, 1993, pp. 508–511.

[11] B. Vucetic and J. Yuan, *Space-Time Coding.* John Wiley & Sons Inc., 2003.

[12] V. Tarokh, N. Seshadri, and A. R. Calderbank, "Space-time codes for high data rate wireless communication: Performance criterion and code construction," *IEEE Trans. Inf. Theory*, vol. 44, no. 2, pp. 744–765, Mar. 1998.

[13] V. Tarokh, H. Jafarkhani, and A. R. Calderbank, "Space-time block codes from orthogonal designs," *IEEE Trans. Inf. Theory*, vol. 45, no. 5, pp. 1456–1467, July 1999.

[14] H. Jafarkhani, *Space-Time Coding: Theory And Practice*. Cambridge Univ. Pr., 2005.

[15] A. Paulraj, R. Nabar, and D. Gore, *Introduction To Space-Time Wireless Communications*. Cambridge Univ. Pr., 2003.

[16] S. M. Alamouti, "A simple transmit diversity technique for wireless communications," *IEEE J. Sel. Areas Commun.*, vol. 16, no. 8, pp. 1451–1458, Oct. 1998.

[17] A. Sendonaris, E. Erkip, and B. Aazhang, "User cooperation diversity. Part I. System description," *IEEE Trans. Commun.*, vol. 51, no. 11, pp. 1927–1938, Nov. 2003.

[18] A. Sendonaris, E. Erkip, B. Aazhang, Q. Inc, and C. Campbell, "User cooperation diversity. Part II. Implementation aspects and performance analysis," *IEEE Trans. Commun.*, vol. 51, no. 11, pp. 1939–1948, Nov. 2003.

[19] J. N. Laneman, D. N. C. Tse, and G. W. Wornell, "Cooperative diversity in wireless networks: Efficient protocols and outage behavior," *IEEE Trans. Inf. Theory*, vol. 50, no. 12, pp. 3062–3080, Dec. 2004.

[20] T. Hunter and A. Nosratinia, "Cooperation diversity through coding," in *Proc. IEEE ISIT*, 2005, p. 220.

[21] ——, "Diversity through coded cooperation," *IEEE Trans. Wireless Commun.*, vol. 5, no. 2, pp. 283–289, 2006.

[22] R. Nabar, H. Bolcskei, and F. Kneubuhler, "Fading relay channels: Performance limits and space-time signal design," *IEEE J. Sel. Areas Commun.*, vol. 22, no. 6, pp. 1099–1109, 2004.

[23] M. Yu and J. Li, "Is amplify-and-forward practically better than decode-and-forward or vice versa?" in *Proc. IEEE ICASSP*, vol. 3, 2005.

[24] M. Simon and M. Alouini, *Digital Communication Over Fading Channels*. Wiley-IEEE Pr., 2005.

[25] M. Uysal, "Diversity analysis of space-time coding in cascaded Rayleigh fading channels," *IEEE Commun. Lett.*, vol. 10, no. 3, pp. 165–167, Mar. 2006.

[26] ——, "Maximum achievable diversity order for cascaded Rayleigh fading channels," *IET Electron. Lett.*, vol. 41, no. 23, pp. 1289–1290, 2005.

[27] A. Papoulis and S. U. Pillai, *Probability, Random Variables, And Stochastic Processes*, 4th ed. McGraw-Hill, New York, 2002.

[28] H. Muhaidat and M. Uysal, "Non-coherent and mismatched-coherent receivers for distributed STBC's with amplify-and-forward relaying," *IEEE Trans. Wireless Commun.*, vol. 6, no. 11, pp. 4060–4070, Nov. 2007.

[29] D. Gu and C. Leung, "Performance analysis of transmit diversity scheme with imperfect channel estimation," *IEEE Electron. Lett.*, vol. 39, no. 4, pp. 402–403, Feb. 2003.

[30] J. K. Cavers, "An analysis of pilot symbol assisted modulation for rayleigh fading channels," *IEEE Trans. Veh. Technol.*, vol. 40, pp. 686–693, Nov. 1991.

[31] Y. Chen and N. Beaulieu, "Optimum pilot symbol assisted modulation," *IEEE Trans. Commun.*, vol. 55, no. 8, pp. 1536–1546, 2007.

[32] Y. Kim, C. Kim, G. Jeong, Y. Bang, H. Park, and S. Choi, "New Rayleigh fading channel estimator based on PSAM channel sounding technique," in *Proc. IEEE ICC*, vol. 3, 2002, pp. 1518–1520.

[33] S. Sampei and T. Sunaga, "Rayleigh fading compensation for QAM in land mobile radio communications," *IEEE Trans. Veh. Technol.*, vol. 42, no. 2, pp. 137–147, 2002.

[34] X. Tang, M. S. Alouini, and A. Goldsmith, "Effect of channel estimation error on M-QAM BER performance inRayleigh fading," *IEEE Trans. Commun.*, vol. 47, no. 12, pp. 1856–1864, Dec. 1999.

[35] M. J. Taghiyar, S. Muhaidat, and J. Liang, "On pilot-symbol-assisted cooperative systems with cascaded Rayleigh and Rayleigh fading channels with imperfect CSI," *J. Sel. Areas Commun. (JSAT)*, pp. 24–31, 2010.

[36] ——, "On the performance of pilot symbol assisted modulation for cooperative systems with imperfect channel estimation," in *Proc. IEEE WCNC*, 2010, pp. 1–5.

[37] P. Larsson, N. Johansson, and K. Sunell, "Coded bi-directional relaying," in *Proc. 63rd IEEE VTC-Spring*, vol. 2, 2006, pp. 851–855.

[38] B. Rankov and A. Wittneben, "Spectral efficient protocols for half-duplex fading relay channels," *IEEE J. Sel. Areas Commun.*, vol. 25, no. 2, pp. 379–389, 2007.

[39] K. Hwang, Y. Ko, and M. Alouini, "Performance bounds for two-way amplify-and-forward relaying based on relay path selection," in *Proc. 69th IEEE VTC-Spring*, 2009, pp. 1–5.

[40] H. Ding, J. Ge, D. Costa, and Z. Jiang, "Outage performance of fixed-gain bidirectional opportunistic relaying in Nakagami-m fading," *IET Electron. Lett.*, vol. 46, no. 18, pp. 1297–1299, 2010.

[41] M. Ju and I. Kim, "Relay selection with analog network coding in bidirectional networks," in *Proc. 25th IEEE QBSC*, 2010, pp. 293–296.

[42] ——, "Joint relay selection and opportunistic source selection in bidirectional cooperative diversity networks," *IEEE Trans. Veh. Technol.*, vol. 59, no. 6, pp. 2885–2897, 2010.

[43] M. J. Taghiyar, S. Muhaidat, and J. Liang, "Relay selection in bidirectional cooperative networks with imperfect channel estimation," *submitted to IEEE Trans. Wireless Commun.*, 2010.

[44] M. Abramowitz and I. Stegun, *Handbook Of Mathematical Functions With Formulas, Graphs, And Mathematical Tables*. Dover Pub., 1964.

[45] H. Suraweera, M. Soysa, C. Tellambura, and H. Garg, "Performance analysis of partial relay selection with feedback delay," *IEEE Signal Process. Lett.*, vol. 17, no. 6, pp. 531–534, 2010.

[46] G. Amarasuriya, C. Tellambura, and M. Ardakani, "Feedback delay effect on dual-hop mimo af relaying with antenna selection," in *Proc. IEEE GLOBECOM*, 2010.

[47] H. Suraweera, T. Tsiftsis, G. Karagiannidis, and M. Faulkner, "Effect of feedback delay on downlink amplify-and-forward relaying with beamforming," in *Proc. IEEE GLOBECOM*, 2010, pp. 1–6.

[48] I. Gradshteyn, I. Ryzhik, A. Jeffrey, D. Zwillinger, and S. Technica, *Table Of Integrals, Series, And Products*. Academic Pr., New York, 1965, vol. 1980.